

# Jam1a–Jam2a interactions regulate haematopoietic stem cell fate through Notch signalling

Isao Kobayashi<sup>1</sup>, Jingjing Kobayashi-Sun<sup>1</sup>, Albert D. Kim<sup>1</sup>, Claire Pouget<sup>1</sup>, Naonobu Fujita<sup>2</sup>, Toshio Suda<sup>3</sup> & David Traver<sup>1,2</sup>

**Notch signalling plays a key role in the generation of haematopoietic stem cells (HSCs) during vertebrate development<sup>1–3</sup> and requires intimate contact between signal-emitting and signal-receiving cells, although little is known regarding when, where and how these intercellular events occur. We previously reported that the somitic Notch ligands, Dlc and Dld, are essential for HSC specification<sup>4</sup>. It has remained unclear, however, how these somitic requirements are connected to the later emergence of HSCs from the dorsal aorta. Here we show in zebrafish that Notch signalling establishes HSC fate as their shared vascular precursors migrate across the ventral face of the somite and that junctional adhesion molecules (JAMs) mediate this required Notch signal transduction. HSC precursors express *jam1a* (also known as *fli1r*) and migrate axially across the ventral somite, where Jam2a and the Notch ligands Dlc and Dld are expressed. Despite no alteration in the expression of Notch ligand or receptor genes, loss of function of *jam1a* led to loss of Notch signalling and loss of HSCs. Enforced activation of Notch in shared vascular precursors rescued HSCs in *jam1a* or *jam2a* deficient embryos. Together, these results indicate that Jam1a–Jam2a interactions facilitate the transduction of requisite Notch signals from the somite to the precursors of HSCs, and that these events occur well before formation of the dorsal aorta.**

JAM proteins belong to the immunoglobulin superfamily of cell adhesion molecules, comprised of three closely related members, JAM1 (also known as JAM-A or F11R), JAM2 (also known as JAM-B), and JAM3 (also known as JAM-C)<sup>5</sup>. It has been reported that Jam1 is expressed in both murine and zebrafish HSC fractions<sup>6,7</sup>, although its role in haematopoiesis remains unknown. In zebrafish, the *jam1* gene was tandemly duplicated on chromosome 5 to generate *jam1a* and *jam1b* (also known as *fli1rl*). The structure of Jam1a is similar to that of human JAM1, which is composed of two immunoglobulin-like domains, a transmembrane domain (TM), and a PDZ-binding domain (PBD), whereas Jam1b lacks the TM and PBD (Extended Data Fig. 1a–d). We therefore focused on Jam1a to determine its potential roles in HSC development. We first examined the expression of *jam1a* in zebrafish embryos. At 14 h post-fertilization (hpf), *jam1a* was expressed in bilateral stripes of posterior lateral mesoderm (PLM) (Extended Data Fig. 2a), which gives rise to both endothelial and haematopoietic lineages<sup>8</sup>. After 18 hpf, however, *jam1a* was no longer detected in endothelial cells (Extended Data Fig. 2b, c). We performed co-staining of *jam1a* with *fli1*, a marker of the vascular lineage. The expression domain of *fli1* overlapped with that of *jam1a* at 14 hpf (Extended Data Fig. 2d), indicating that PLM cells indeed express *jam1a* at this stage. We observed the downregulation of *jam1a* in purified green fluorescent protein (GFP)-labelled endothelial cells (*fli1:GFP*<sup>+</sup> cells) from 14 to 20 hpf (Extended Data Fig. 2e).

To determine if HSC precursors are contained within *jam1a*<sup>+</sup> PLM cells, we performed lineage tracing using the combined transgenic lines, *-2.2jam1a:CreER*<sup>T2</sup>, which expresses *CreER*<sup>T2</sup> under the control of *jam1a* regulatory elements, and *bactin2:loxP-BFP-loxP-DsRed*, which switches from expression of blue fluorescent protein (BFP) to the DsRed red fluorescent protein following Cre-based recombination (Fig. 1a, Extended Data Fig. 2f). Double-transgenic embryos were treated with

4-hydroxytamoxifen (4OHT) following two different schedules (Fig. 1b). An ‘early’ group was treated with 4OHT from 8 hpf, a stage before PLM formation<sup>9</sup>, and a ‘late’ group from 30 hpf, a stage just before HSC emergence in the dorsal aorta<sup>10,11</sup>. These embryos were grown to 3–5 months of age, after which whole kidney marrow cells were analysed by flow cytometry (Fig. 1c). As shown in Fig. 1d, high percentages of ‘switched’ DsRed<sup>+</sup> cells were detected in the ‘early’ group. DsRed<sup>+</sup> cells were comprised of multiple types of blood lineages (Fig. 1e). In contrast to the ‘early’ schedule, DsRed<sup>+</sup> cells were nearly undetectable in the ‘late’ group (Fig. 1d). These results indicate that *jam1a* is expressed in the shared vascular precursors of HSCs during early somitogenesis stages. The expression of *jam1a* in HSC precursors was further confirmed by additional lineage-tracing studies using a *-5.1jam1a:CreER*<sup>T2</sup> transgenic animal, which has an extended *jam1a* promoter/enhancer region (Extended Data Fig. 2g–l).

To examine the function of Jam1a in haematopoiesis, we designed two different morpholino oligonucleotides (MOs), *jam1a* MOatg (a translation-blocking MO) and MOex7 (a splice-blocking MO) (Extended Data Fig. 3a–e). We first examined the expression of the HSC marker gene *runx1* in these morphants. As shown in Fig. 1f, *runx1* was detected in the dorsal aorta in uninjected wild-type embryos at 26 hpf. In contrast, *runx1* was nearly undetectable in *jam1a* MOatg- and MOex7-injected embryos at the same stage (Fig. 1g, h). The expression of *efnb2a* (ephrin-B2a, a dorsal aorta marker gene) was unaffected in either morphant (Fig. 1i–k), suggesting that the dorsal aorta is specified normally. To further characterize *jam1a* morphants, we investigated the expression of additional marker genes. The expression of *cmyb* (another HSC marker) in the dorsal aorta was largely absent in *jam1a* morphants (Fig. 1l, m, Extended Data Fig. 3f, g). T-cell colonization of the thymus requires input from HSCs, providing a useful readout for whether HSCs have been specified or not. In *jam1a* morphants, the expression of *rag1* (a marker of immature T cells) was absent in the thymus at 4 days post-fertilization (dpf) (Fig. 1n, o, Extended Data Fig. 3h, i). A truncated isoform of *scl* (also known as *tall1*), *scl-β*, has been shown to mark haemogenic endothelium in the dorsal aorta<sup>12</sup>. Comparison of *scl-α/β* and *scl-α* probes revealed the specific reduction of *scl-β* in the dorsal aorta in *jam1a* morphants (Fig. 1p–s). Nascent HSCs can be visualized as *cmyb:GFP*; *kdr:lmCherry* double-positive cells in the ventral floor of the dorsal aorta<sup>10</sup>. The number of double-positive cells in the dorsal aorta was twelve times lower in *jam1a* morphants than in wild-type embryos (Extended Data Fig. 4a–c). The expression of *gata1* (an erythroid marker) and *l-plastin* (a myeloid marker) at 24 hpf was normal in *jam1a* morphants, whereas the expression of *l-plastin* at 4 dpf was reduced in the caudal haematopoietic tissue (CHT) (Extended Data Fig. 4d–f). These results indicate that primitive haematopoiesis is unaffected, but definitive haematopoiesis is defective in *jam1a* morphants. The vasculature in the trunk was normal in *jam1a* morphants, whereas development of the vascular plexus in the CHT was slightly abnormal (Extended Data Fig. 4g–j). Development of the pronephros, somite, sclerotome and notochord was unaffected in *jam1a* morphants (Extended Data Fig. 4k–o). These results indicate that the failure of HSC specification in *jam1a* morphants is specific and not due to gross

<sup>1</sup>Department of Cellular and Molecular Medicine, University of California, San Diego, La Jolla, California 92093-0380, USA. <sup>2</sup>Section of Cell and Developmental Biology, University of California, San Diego, La Jolla, California 92093-0380, USA. <sup>3</sup>Department of Cell Differentiation, The Sakaguchi Laboratory, School of Medicine, Keio University, Shinjuku, Tokyo 160-8582, Japan.

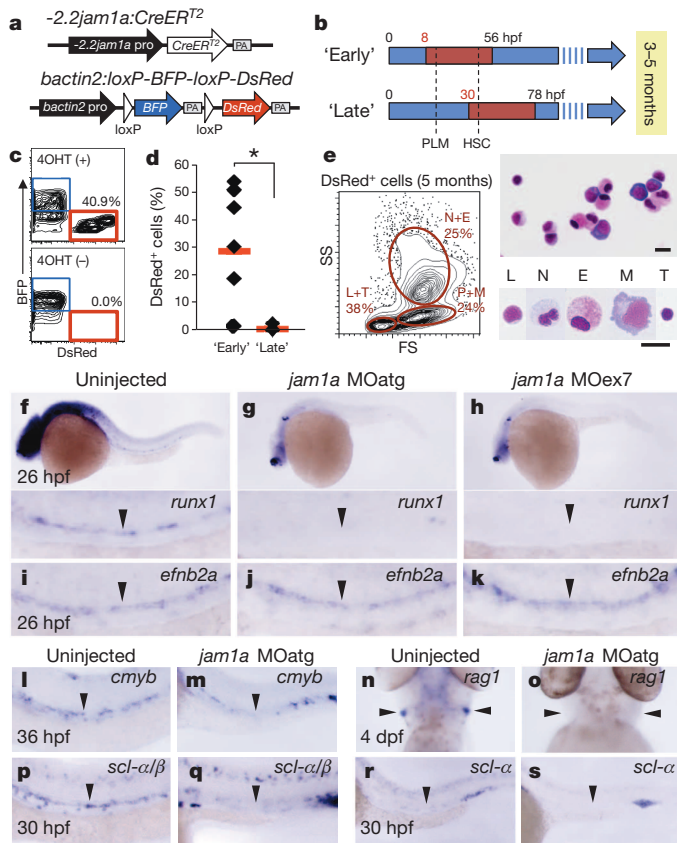


**Figure 1 | Loss of *jam1a* results in the loss of HSCs.** **a**, Vector constructs of transgenic animals used for lineage tracing. PA, polyA. **b**, Two different schedules of 4-hydroxytamoxifen (4OHT) treatment ('early' and 'late'). Red insets in the blue arrows indicate the period of the 4OHT treatment. **c**, Flow cytometric analysis of adult kidney marrow cells. **d**, The percentages of DsRed<sup>+</sup> cells in kidney marrow in the 'early' ( $n = 7$ ) or 'late' group ( $n = 10$ ). Red bars indicate the mean percentage. \* $P < 0.002$ , by Student's *t*-test. **e**, Flow cytometric and morphological analysis of DsRed<sup>+</sup> cells. L, lymphocytes, N, neutrophils; E, eosinophils; M, monocytes; T, thrombocytes, P, precursors. **f–k**, Expression of *runx1* and *efnb2a* in uninjected, *jam1a* MOatg-, or MOex7-injected embryos. **l–s**, Expression of *cmyb*, *rag1*, *scl-α/β*, and *scl-α* in uninjected or *jam1a* MOatg-injected embryos. Arrowheads indicate the dorsal aorta (**f–m**, **p–s**) or thymus (**n**, **o**). Data are pooled from two independent experiments (**c–e**) or representative of two independent experiments with two different clutches of embryos (**f–s**).

malformations in adjacent environmental tissues. The effects of MOs are summarized in Supplementary Table 1.

Since *jam1a* is expressed in PLM cells, we next examined the formation and migration of the PLM in *jam1a* morphants. The expression of *fli1* at 12 hpf was normal in both types of *jam1a* morphants (Fig. 2a–c), suggesting that PLM formation is unaffected. PLM cells migrate axially and reach the midline by 17 hpf (Fig. 2d). We observed a delay in the migration of PLM cells in both types of *jam1a* morphants, in that a subset of *fli1*<sup>+</sup> cells did not reach the midline by 17 hpf (Fig. 2e, f). We performed time-lapse imaging of PLM cells from 14 hpf using *fli1*:*GFP*; *phldb1*:*mCherry* double transgenic embryos, where endothelial precursors and somitic cells are labelled by GFP and mCherry expression, respectively. PLM cells in the first wave reached the midline by 15.5 hpf in wild-type embryos, whereas the remaining cells reached the midline by 17.5 hpf to form the 'vascular cord' (Fig. 2g, Supplementary Video 1). In *jam1a* morphants, however, only a few PLM cells reached the midline by 15.5 hpf. Moreover, some PLM cells remained at the lateral borders of the somites at 17.5 hpf, and the vascular cord was discontinuous (Fig. 2h, Supplementary Videos 2 and 3). We examined the morphology of migrating PLM cells. In wild-type embryos, most migrating *fli1*:*GFP*<sup>+</sup> PLM cells displayed a flattened morphology

and appeared to interact closely with the ventral domain of the somite (Fig. 2i). By contrast, PLM cells in *jam1a* morphants displayed a round shape with relatively little surface contact with the somite (Fig. 2j).

To exclude the possibility of a general developmental delay in *jam1a* morphants, we enumerated somites at 14 hpf in *jam1a* MO control- and MOatg-injected embryos. We mainly observed nine somites formed in both *jam1a* MO control- and *jam1a* MOatg-injected embryos at this stage, and there was no significant difference in the average numbers of somites between groups (Fig. 2k, l). This indicates that the migration defect observed in *jam1a* morphants is specific and not due to developmental delay. In zebrafish, Hedgehog (Hh) and Vascular endothelial growth factor a (Vegfa) signalling pathways have been implicated to regulate the migration of PLM cells<sup>13,14</sup>. In *jam1a* morphants, however, the expression of *shha* (sonic hedgehog a) and *vegfa* as well as their downstream target *efnb2a* was unaffected (Fig. 1i–k, Extended Data Fig. 4n–q), indicating that the defect of PLM cell migration in *jam1a* morphants is independent of the Hh and Vegfa signalling pathways.

Because PLM cells migrate along the ventral domain of the somites, which includes the sclerotome, it is likely that a binding partner of Jam1a is expressed on the somitic epithelium. Previous studies determined the expression patterns of zebrafish *jam* genes and their physical binding properties by surface plasmon resonance. These studies showed that Jam1a can bind to Jam2a, Jam2b and Jam3a, but not to Jam1a (homotypically), Jam1b or Jam3b. Moreover, among these 6 *jam* genes, only *jam2a* and *jam3b* are expressed in somites<sup>15,16</sup>. Therefore, we next investigated whether PLM cells make contact with *jam2a*<sup>+</sup> somitic cells. As shown in Fig. 3a, *jam2a* was specifically expressed in somites at 16 hpf, a stage when PLM cells are migrating. Quantitative polymerase chain reaction (qPCR) results also showed that *jam2a* was highly expressed in purified *alpha-actin*:*GFP*<sup>+</sup> somitic cells at 14 hpf, whereas *jam1a* was highly expressed in purified *fli1*:*GFP*<sup>+</sup> PLM cells (Fig. 3b). Histological analysis of 16 hpf embryos revealed that migrating *fli1*:*GFP*<sup>+</sup> PLM cells were in close contact with *jam2a*<sup>+</sup> somitic cells (Fig. 3c).

To determine if Jam1a can bind to Jam2a, we performed coimmunoprecipitation experiments using transiently transfected Flag-tagged Jam1a (Jam1a-Flag) and haemagglutinin-tagged Jam2a (Jam2a-HA) constructs in HEK293T cells. Anti-Flag immunoprecipitation followed by anti-HA western blotting showed specific binding of Jam1a to Jam2a (Fig. 3d). To further test their interaction, we used a Duolink proximity ligation assay (PLA), which can demonstrate protein–protein interactions *in situ* by eliciting a fluorescent signal (Fig. 3e). As shown in Fig. 3f, PLA signals were detected in the boundary region between transfected Jam1a-Flag<sup>+</sup> cells and Jam2a-HA<sup>+</sup> cells, revealing the interaction of these proteins *in trans*. These results suggest that cells of PLM maintain intimate contact with cells of the ventral somite via Jam1a–Jam2a interactions during their migration.

This model predicts that loss of *jam2a* function would phenocopy the effects in *jam1a* morphants. We thus examined both HSC specification and PLM cell migration in *jam2a* MOatg- or MOex5-injected embryos (Extended Data Fig. 5a–d). The expression of *runx1* in the dorsal aorta was greatly reduced in both *jam2a* morphants, whereas *efnb2a* expression was unaffected (Fig. 3g–j, Extended Data Fig. 5e–l). In addition, axial migration of PLM cells was greatly delayed in both types of *jam2a* morphants (Fig. 3k, Supplementary Videos 4 and 5), despite only a modest delay in development (Fig. 3l). Migrating *fli1*:*GFP*<sup>+</sup> PLM cells in *jam2a* morphants displayed a round shape (Extended Data Fig. 5m), similar to that shown in *jam1a* morphants (Fig. 2j). The average contact surface area between a PLM cell and the somite was significantly reduced in both *jam1a* and *jam2a* morphants compared with uninjected embryos (Extended Data Fig. 5n). The effects of *jam2a* MOs were further validated in *jam2a* mutants (*jam2a*<sup>hu3319</sup>). Approximately 80% of homozygous *jam2a*<sup>hu3319</sup> embryos showed nearly undetectable expression of *runx1* and *cmyb* in the dorsal aorta and *rag1* in the thymus (Extended Data Fig. 6a–g). Moreover, approximately 85% of homozygous *jam2a*<sup>hu3319</sup> embryos showed delayed PLM cell migration compared with wild-type embryos (Extended Data Fig. 6h, i). Formation of the vasculature, however, was grossly normal

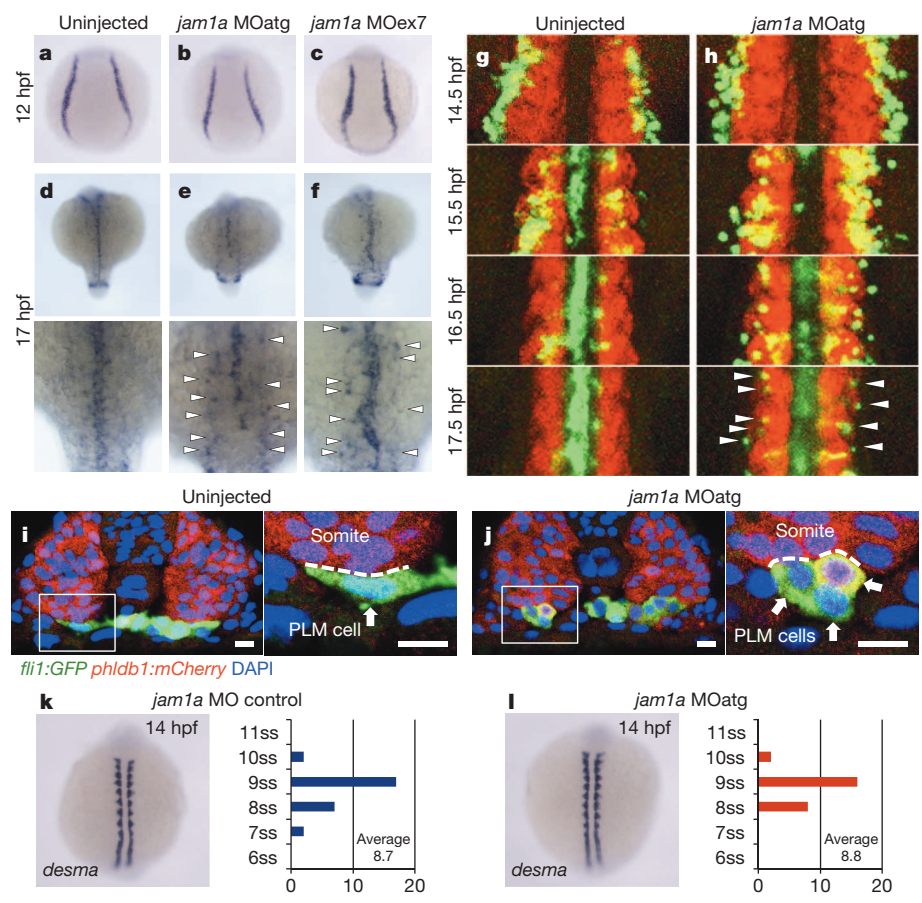


**Figure 2 | PLM cell migration is delayed in *jam1a* morphants.** **a–f**, The expression of *fli1* in uninjected, *jam1a* MOatg-, or MOex7-injected embryos. Arrowheads indicate a subset of *fli1*<sup>+</sup> cells that did not reach the midline by 17 hpf. **g, h**, Time-lapse images of *fli1:GFP*; *phldb1:mCherry* double-transgenic embryos. The regions from the tenth to twelfth somite are shown at each time point. Arrowheads indicate a subset of *fli1:GFP*<sup>+</sup> cells that did not reach the midline. **i, j**, Transverse sections of *fli1:GFP*; *phldb1:mCherry* embryos uninjected (15.5 hpf) or injected with *jam1a* MOatg (16 hpf). High magnification views of the boxed regions are shown in the right panels. Dotted lines indicate the contact surface area between PLM cells (arrows) and somitic cells. Bars, 10  $\mu$ m. **k, l**, The number of somites was counted in *jam1a* MO control- or MOatg-injected embryos at 14 hpf based on the expression of *desma*. The average numbers of somites in embryo groups are shown on each graph. There was no significant difference between *jam1a* MO control- ( $n = 28$ ) and MOatg-injected embryos ( $n = 26$ ,  $P = 0.61$ , by Student's *t*-test). ss, somite-stage. Data are representative of two independent experiments with two different clutches of embryos (**a–f, k, l**) or three embryos (**i, j**) or three independent experiments with nine embryos (**g, h**).

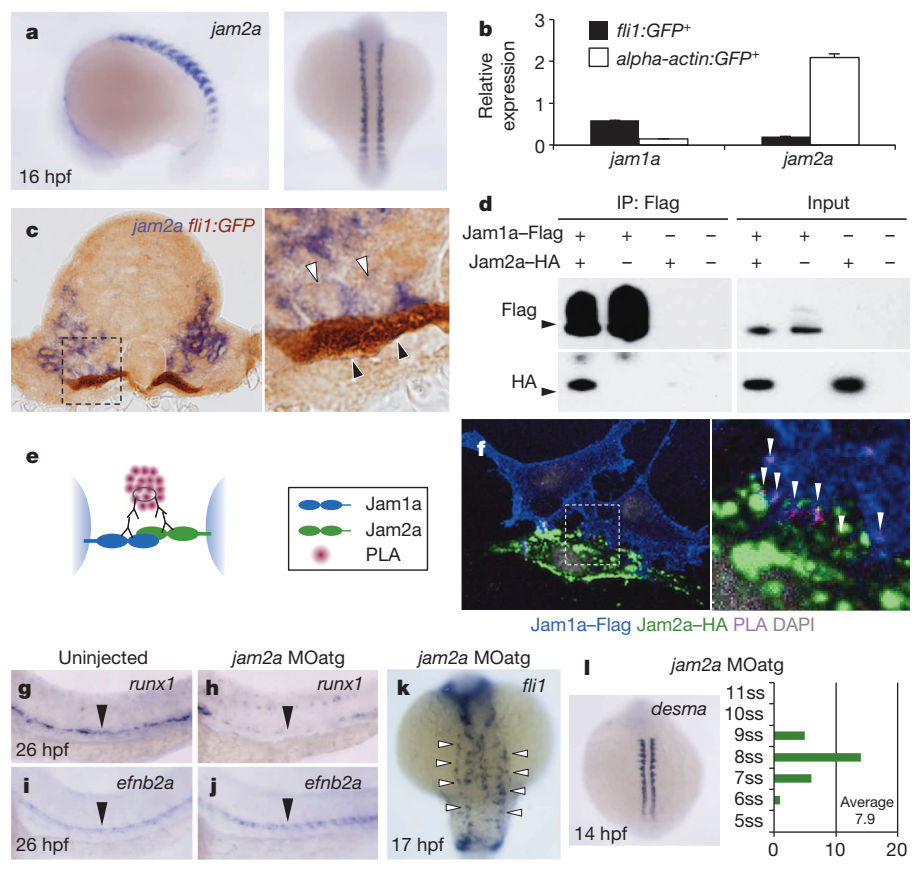


**Figure 3 | Loss of somitic *jam2a* phenocopies the *Jam1a* defect.** **a**, Expression of *jam2a* at 16 hpf. **b**, Relative expression levels of *jam1a* and *jam2a* in purified *fli1:GFP*<sup>+</sup> and *alpha-actin:GFP*<sup>+</sup> cells at 14 hpf. Error bars, s.d. **c**, A transverse section of a *fli1:GFP* embryo stained with *jam2a* (purple, white arrowheads) and anti-GFP antibody (brown, black arrowheads) at 16 hpf. The right panel shows a high magnification view of the boxed region. **d**, Co-immunoprecipitation (Co-IP) using anti-Flag antibody. The immunoprecipitates were examined by western blotting using anti-Flag or anti-HA antibody. Inputs represent 10% of cell lysates used in the Co-IP experiment. Arrowheads indicate 40 kDa. **e**, A schematic diagram of the proximity ligation assay (PLA). **f**, A representative result of Duolink PLA. The right panel represents a high magnification view of the boxed region. Arrowheads indicate PLA signal. **g–j**, The expression of *runx1* and *efnb2a* in uninjected or *jam2a* MOatg-injected embryos. Arrowheads indicate the dorsal aorta. **k**, The expression of *fli1* in *jam2a* MOatg-injected embryo at 17 hpf. Arrowheads indicate a subset of *fli1*<sup>+</sup> cells that did not reach the midline. **l**, The number of somites was counted in *jam2a* MOatg-injected embryos ( $n = 26$ ) at 14 hpf based on the expression of *desma*. Average somite number is shown on the graph. ss, somite-stage. Data are representative of two independent experiments with two different clutches of embryos (**a–c, g–l**) or three independent experiments (**d, f**).

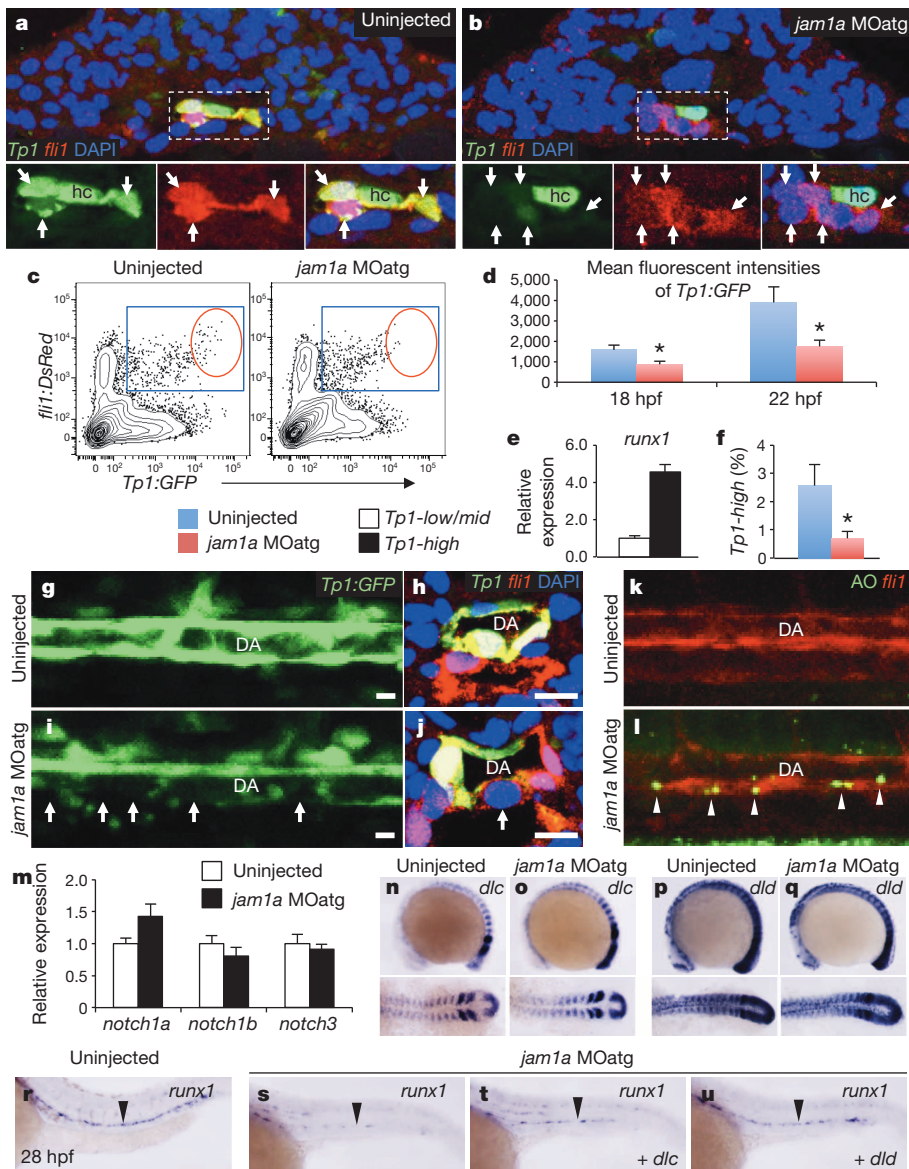


**Figure 4 | Notch signalling is depleted in *jam1a* morphants.** **a, b**, Transverse sections of *Tp1:GFP*; *fli1:DsRed* embryos uninjected or injected with *jam1a* MOatg at 18 hpf. Green and red channels and merges of the boxed regions are shown in the lower panels. Arrows indicate *fli1:DsRed*<sup>+</sup> cells. hc, hypochord. **c–f**, Flow cytometric and gene expression analysis of *Tp1:GFP*; *fli1:DsRed* embryos. Representative results of flow cytometric analysis at 22 hpf (**c**), the mean fluorescent intensities of GFP in *Tp1:GFP*<sup>+</sup>; *fli1:DsRed*<sup>+</sup> populations (**d**), relative expression levels of *runx1* in the *Tp1:GFP*<sup>high</sup> and *Tp1:GFP*<sup>low/mid</sup> population of *fli1:DsRed*<sup>+</sup> cells in wild-type embryos at 22 hpf (**e**), and the percentages of *Tp1:GFP*<sup>high</sup> in *fli1:DsRed*<sup>+</sup> populations at 22 hpf (**f**) are shown. Blue gates and red circles indicate the *Tp1:GFP*<sup>+</sup>; *fli1:DsRed*<sup>+</sup> and *Tp1:GFP*<sup>high</sup>; *fli1:DsRed*<sup>+</sup> population, respectively. \**P* < 0.01, by Student's *t*-test. Error bars, s.d. **g–j**, Lateral views of the dorsal aorta (DA) in *Tp1:GFP* embryos and transverse sections of *Tp1:GFP*; *fli1:DsRed* embryos uninjected or injected with *jam1a* MOatg at 28 hpf. Arrows indicate relatively low activation of *Tp1:GFP* in the ventral floor of the DA. Bars, 10 μm. **k, l**, Acridine orange (AO) staining under the *fli1:DsRed* background in uninjected or *jam1a* MOatg-injected embryos at 30 hpf. Arrowheads indicate AO-stained apoptotic cells. **m**, Relative expression levels of *notch1a*, *notch1b*, and *notch3* in purified *fli1:GFP*<sup>+</sup> cells obtained from uninjected or *jam1a* MOatg-injected embryos at 18 hpf. Error bars, s.d. **n–q**, The expression of *dlc* and *dld* in uninjected or *jam1a* MOatg-injected embryos at 14 hpf. **r–u**, The expression of *runx1* at 26 hpf. Embryos were uninjected, injected with *jam1a* MOatg alone, or co-injected with *jam1a* MOatg and *dlc* or *dld* mRNA. Data are representative of two independent experiments with four embryos (**a, b, h, j**), eight embryos (**g, i, k, l**), four different clutches of embryos (**c–f**), or two different clutches of embryos (**m–u**).

in *jam2a*<sup>hu3319</sup> embryos (Extended Data Fig. 6j–o). These phenotypes are consistent with those in *jam1a* morphants, suggesting that Jam1a–Jam2a interactions are involved in both PLM cell migration and HSC specification.

Despite a large reduction in embryonic HSC number, approximately 50% of homozygous *jam2a*<sup>hu3319</sup> animals were viable and showed almost normal haematopoiesis in the adult kidney (Extended Data Fig. 6p, q). Further studies will be required to understand how haematopoiesis can recover in *jam2a*<sup>hu3319</sup> animals during development. Perhaps related to this observation, a dispensable role for Jam2 in adult haematopoiesis has also been reported in mice<sup>17,18</sup>.

To better understand how both *jam1a* and *jam2a* morphants show impaired HSC specification, we considered possible signal transduction mechanisms from the somite. Because our recent work demonstrated that two somitic Notch ligands, Dlc and Dld, are essential for HSC specification<sup>4</sup>, and because Notch is a juxtacrine signal that requires close contact between adjacent cells, we prioritized analysis of the Notch signalling pathway. To test the hypothesis that Jam1a–Jam2a interactions facilitate Notch signal transmission between the PLM and somite, we first examined the activation of Notch signalling in *jam1a* morphants using a Notch reporter line, *Tp1:GFP*, which expresses GFP under the control of tandem Notch responsive elements<sup>19</sup>. In wild-type embryos,

some *fli1:DsRed*<sup>+</sup> endothelial cells strongly expressed *Tp1:GFP* in the midline at 18 hpf (Fig. 4a). In *jam1a* morphants, by contrast, most of the *fli1:DsRed*<sup>+</sup> cells showed weak or no expression of the *Tp1:GFP* reporter at the same stage (Fig. 4b). The expression levels of *Tp1:GFP* in *fli1:DsRed*<sup>+</sup> cells were further quantified by flow cytometry (Fig. 4c). The mean fluorescence intensity of GFP in the *Tp1:GFP*<sup>+</sup>; *fli1:DsRed*<sup>+</sup> population was significantly lower in *jam1a* morphants than in uninjected embryos (Fig. 4d). In wild-type embryos, *runx1* is highly expressed in the *Tp1:GFP*<sup>high</sup> fraction of *fli1:DsRed*<sup>+</sup> cells at 22 hpf (Fig. 4e), suggesting that HSC precursors are enriched in this population. Notably, the percentage of *Tp1:GFP*<sup>high</sup>; *fli1:DsRed*<sup>+</sup> cells was significantly lower in *jam1a* morphants (Fig. 4f). At 28 hpf, *Tp1:GFP* was highly expressed in the dorsal aorta in wild-type embryos (Fig. 4g, h). Interestingly, in *jam1a* morphants, *Tp1:GFP* expression was weak and discontinuous along the floor of the dorsal aorta (Fig. 4i, j), the site of HSC emergence<sup>10,11</sup>. In addition, we observed many apoptotic cells along the aortic floor in *jam1a* morphants (Fig. 4k, l), suggesting that, in the absence of Notch signalling, HSC precursors fail to be specified and undergo apoptosis.

To test whether ectopic activation of Notch signalling is sufficient to rescue HSCs in *jam1a* morphants, we enforced expression of the Notch intracellular domain (NICD), a dominant activator of the Notch pathway<sup>3</sup>, using combined *hsp70:Gal4*; *UAS:NICD* transgenic lines. Heat-shock

induction of NICD at 14 hpf rescued the expression of *runx1* in the dorsal aorta in *jam1a* morphants (Extended Data Fig. 7a, b), similar to that shown previously for rescue of *mind bomb* (*mib*) mutants or *wnt16* morphants<sup>3,4</sup>. The expression of *runx1* was also rescued in *jam1a* morphants when NICD was induced in the PLM using the *fli1:Gal4* line (Extended Data Fig. 7c, d). Similar results were obtained in *jam2a* MOatg-injected embryos (Extended Data Fig. 7e, f).

At 15 hpf, migrating *fli1:GFP*<sup>+</sup> cells were observed to make direct contact with *dlc*<sup>+</sup> or *dld*<sup>+</sup> somitic cells (Extended Data Fig. 8a, b), indicating that PLM cells may receive Notch signalling via presentation of somitic Notch ligands. We observed low activation of *Tp1:GFP* in endothelial cells in *wnt16* morphants (Extended Data Fig. 8c–g), which show a reduction in somitic *dlc* and *dld*<sup>+</sup>. This suggests that Notch signalling in endothelial cells is activated at least in part by somitic Dlc and/or Dld. We investigated the expression of somitic Notch ligand genes (*dlc* and *dld*) as well as aortic Notch receptor and ligand genes (*notch1a*, *notch1b*, *notch3*, *dlc* and *delta-like 4* (*dll4*)) in *jam1a* morphants. Importantly, each was expressed normally in *jam1a* morphants (Fig. 4m–q, Extended Data Fig. 9a–h), suggesting that the defect in Notch signalling in *jam1a* morphants is due to low Notch signal transmission rather than to misregulation of Notch signalling components. Consistent with this postulate, we observed less contact surface area between migrating PLM cells and the somite in both *jam1a* and *jam2a* morphants (Fig. 2i, j, Extended Data Fig. 5m, n), which correlates with low activation of Notch signalling. Our hypothesis is further supported by an additional rescue experiment in which *dlc* or *dld* is globally overexpressed in *jam1a* morphants to present more Notch ligand to HSC precursors. As presented in Fig. 4u, the expression of *runx1* in the dorsal aorta was almost fully rescued by co-injection of *dld* messenger RNA (mRNA) along with the *jam1a* MOatg, whereas *runx1* expression was only partially rescued following co-injection with *dlc* mRNA (Fig. 4r–u). Furthermore, the expression of *Tp1:GFP* was also restored in the ventral floor of the dorsal aorta by co-injection with *dlc* or *dld* mRNA (Extended Data Fig. 9i–p). These data confirm that the impairment of HSC specification in *jam1a* morphants is caused by inadequate activation of Notch signalling in HSC precursors and suggest that Jam1a and Jam2a normally mediate the physical interaction between these precursors and the somite, which is required for efficient Notch signal transmission (Extended Data Fig. 10).

It has been reported that the overall levels of Notch signal transmission is proportional to adhesion strength between Notch receptor- and ligand-expressing cells<sup>20</sup>. Our data demonstrate that *runx1* is highly expressed in the *Tp1:GFP*<sup>high</sup> population of endothelial cells (Fig. 4e), suggesting that a relatively high level of Notch signalling is required to generate HSC fate. These findings strongly suggest that efficient Notch signal transduction in HSC precursors requires intimate intercellular contact mediated by Jam proteins. Moreover, our data suggest that HSC fate is established much earlier than previously appreciated, during the axial migration of PLM cells, which is well before formation of the dorsal aorta. These new findings may provide key insights into the timing and tissue interactions needed to instruct HSC fate, which should help inform *in vitro* approaches to generate HSCs from pluripotent stem cells.

## METHODS SUMMARY

For morpholino knockdown experiments, zygotes were injected with 1 nl of morpholino oligonucleotides (MOs, GeneTools). MO concentrations used were: *jam1a* MOatg (100  $\mu$ M), *jam1a* MO control (100  $\mu$ M), *jam1a* MOex7 (300  $\mu$ M), *jam2a* MOatg (300  $\mu$ M), *jam2a* MOex5 (400  $\mu$ M), and *wnt16* MO2 (5 ng nl<sup>-1</sup>). Fluorescent images were captured using an SP5 inverted confocal microscope (Leica) as previously described<sup>10</sup>. Flow cytometry, qPCR, *in situ* hybridization, histology, Duolink PLA, immunoprecipitation, and western blotting were performed as described in the Methods section.

**Online Content** Methods, along with any additional Extended Data display items and Source Data, are available in the online version of the paper; references unique to these sections appear only in the online paper.

Received 24 September 2013; accepted 27 June 2014.

Published online 13 August 2014.

- Hadland, B. K. *et al.* A requirement for Notch1 distinguishes 2 phases of definitive hematopoiesis during development. *Blood* **104**, 3097–3105 (2004).
- Yoon, M. J. *et al.* Mind bomb-1 is essential for intraembryonic hematopoiesis in the aortic endothelium and the subaortic patches. *Mol. Cell. Biol.* **28**, 4794–4804 (2008).
- Burns, C. E., Traver, D., Mayhall, E., Shepard, J. L. & Zon, L. I. Hematopoietic stem cell fate is established by the Notch-Runx pathway. *Genes Dev.* **19**, 2331–2342 (2005).
- Clements, W. K. *et al.* A somitic Wnt16/Notch pathway specifies haematopoietic stem cells. *Nature* **474**, 220–224 (2011).
- Weber, C., Fraemohs, L. & Dejana, E. The role of junctional adhesion molecules in vascular inflammation. *Nature Rev. Immunol.* **7**, 467–477 (2007).
- Sugano, Y. *et al.* Junctional adhesion molecule-A, JAM-A, is a novel cell-surface marker for long-term repopulating hematopoietic stem cells. *Blood* **111**, 1167–1172 (2008).
- Kobayashi, I. *et al.* Comparative gene expression analysis of zebrafish and mammals identifies common regulators in hematopoietic stem cells. *Blood* **115**, e1–e9 (2010).
- Thompson, M. A. *et al.* The cloche and spadetail genes differentially affect hematopoiesis and vasculogenesis. *Dev. Biol.* **197**, 248–269 (1998).
- Jin, S. W., Beis, D., Mitchell, T., Chen, J. N. & Stainier, D. Y. Cellular and molecular analyses of vascular tube and lumen formation in zebrafish. *Development* **132**, 5199–5209 (2005).
- Bertrand, J. Y. *et al.* Haematopoietic stem cells derive directly from aortic endothelium during development. *Nature* **464**, 108–111 (2010).
- Kissa, K. & Herbomel, P. Blood stem cells emerge from aortic endothelium by a novel type of cell transition. *Nature* **464**, 112–115 (2010).
- Qian, F. *et al.* Distinct functions for different *scl* isoforms in zebrafish primitive and definitive hematopoiesis. *PLoS Biol.* **5**, e132 (2007).
- Gering, M. & Patient, R. Hedgehog signaling is required for adult blood stem cell formation in zebrafish embryos. *Dev. Cell* **8**, 389–400 (2005).
- Wilkinson, R. N. *et al.* Hedgehog signaling via a calcitonin receptor-like receptor can induce arterial differentiation independently of VEGF signaling in zebrafish. *Blood* **120**, 477–488 (2012).
- Powell, G. T. & Wright, G. J. Jamb and Jamc are essential for vertebrate myocyte fusion. *PLoS Biol.* **9**, e1001216 (2011).
- Powell, G. T. & Wright, G. J. Genomic organisation, embryonic expression and biochemical interactions of the zebrafish junctional adhesion molecule family of receptors. *PLoS ONE* **7**, e40810 (2012).
- Sakaguchi, T. *et al.* Putative “stemness” gene jam-B is not required for maintenance of stem cell state in embryonic, neural, or hematopoietic stem cells. *Mol. Cell. Biol.* **26**, 6557–6570 (2006).
- Arcangeli, M. L. *et al.* JAM-B regulates maintenance of hematopoietic stem cells in the bone marrow. *Blood* **118**, 4609–4619 (2011).
- Parsons, M. J. *et al.* Notch-responsive cells initiate the secondary transition in larval zebrafish pancreas. *Mech. Dev.* **126**, 898–912 (2009).
- Ahimou, F., Mok, L. P., Bardot, B. & Wesley, C. The adhesion force of Notch with Delta and the rate of Notch signaling. *J. Cell Biol.* **167**, 1217–1229 (2004).

**Supplementary Information** is available in the online version of the paper.

**Acknowledgements** The authors thank G. Wright for providing the *jam2a*<sup>hu3319</sup> line, A. Shimizu for help in generating transgenic lines, M. Osato for providing the *I-SceI-pBSII SK+* vector, M. Distel for providing *phldb1:Gal4-mCherry* animals, and W. Clements, Y. Lee and E. Butko provided critical evaluation of the manuscript. This work was supported in part by a JSPS Research fellowship for Young Scientists and a JSPS Postdoctoral fellowship for Research Abroad (I.K.), by a New Investigator Award from the California Institute of Regenerative Medicine, R01-DK074482 from the National Institutes of Health, and an Innovative Science Award from the American Heart Association (D.T.).

**Author Contributions** I.K., T.S. and D.T. designed research. I.K. generated transgenic lines, performed flow cytometry, cell culture and transfection experiments, analysed data, and wrote the manuscript. I.K. and J.K.-S. performed *in situ* hybridization and real-time PCR. I.K., J.K.-S. and C.P. generated *in situ* probes. I.K. and N.F. performed immunoprecipitation and western blotting. I.K. and A.D.K. performed confocal imaging. J.K.-S. performed histological analyses. A.D.K., C.P., T.S. and D.T. edited the manuscript.

**Author Information** Reprints and permissions information is available at [www.nature.com/reprints](http://www.nature.com/reprints). The authors declare no competing financial interests. Readers are welcome to comment on the online version of the paper. Correspondence and requests for materials should be addressed to D.T. ([dtraver@ucsd.edu](mailto:dtraver@ucsd.edu)).

## METHODS

**Zebrafish husbandry and heat shock.** Zebrafish were maintained as previously described<sup>21</sup> and in accordance with University of California at San Diego Institutional Animal Care and Use Committee (IACUC) guidelines. All animal and cell line experiments are approved by the University of California at San Diego IACUC. The *Tg(cmyb:GFP)<sup>z169</sup>* (ref. 22), *Tg(kdrl:HsHRAS-mCherry)<sup>z896</sup>* (ref. 23), *Tg(fli:GFP)<sup>1</sup>* (ref. 24), *Tg(fli:DsRed)<sup>um13</sup>* (ref. 25), *Et(phldb1:Gal4-mCherry)* (ref. 26), *Tg(alpha-actin:GFP)* (ref. 27), *Tg(Tp1:GFP)<sup>um14</sup>* (ref. 19), *Tg(hsp70:Gal4)<sup>1.5kca4</sup>* (ref. 3), *Tg(UAS:NICD)<sup>kca3</sup>* (ref. 3), *Tg(fli:Gal4)<sup>ubs4</sup>* (ref. 28), and *jam2a<sup>tu3319</sup>* (ref. 15) were used. Heat shocks were performed at 14 hpf for 45 min at 38 °C.

**Alignment and phylogenetic analysis.** cDNA and amino acid sequences were obtained from the National Center for Biotechnology Information (NCBI) database (<http://www.ncbi.nlm.nih.gov/>). The deduced amino acid sequences of zebrafish *Jam1a*, *Jam1b*, and human *JAM1* were aligned using ClustalW (European Bioinformatics Institute). A phylogenetic tree of JAM subfamily proteins was constructed as previously described<sup>29</sup>. Protein domains were predicted using the SMART database (<http://smart.embl-heidelberg.de/>). The gene locations for zebrafish *jam1a* and *jam1b* were examined using the genomic sequence database version 9 at Sanger (<http://www.sanger.ac.uk/>).

**Generation of transgenic lines.** *Tg(-2.2jam1a:GFP)<sup>sd25</sup>*: a 2.2-kb fragment immediately upstream of the *jam1a* transcriptional start site was cloned from zebrafish genomic DNA and ligated upstream of the *EGFP* site in *I-SceI-pBSII SK+*. Vectors were flanked by *I-SceI* sites and injected into one-cell stage embryos with *I-SceI* (Roche, 11362399001) to generate transgenic founders. Three *-2.2jam1a:GFP* founders were identified by screening for the GFP fluorescence of progeny. The line used in this study showed the strongest GFP expression. *Tg(-2.2jam1a:CreER<sup>T2</sup>, -2.2jam1a:GFP)<sup>sd26</sup>*: The *CreER<sup>T2</sup>* fragment was amplified by PCR from *pCAG-CreER<sup>T2</sup>* (Addgene) and ligated upstream of the *jam1a* promoter in the *jam1a:GFP* vector. Then, an additional *jam1a* promoter was ligated upstream of the *CreER<sup>T2</sup>*. Ten *-2.2jam1a:CreER<sup>T2</sup>, -2.2jam1a:GFP* founders were identified by screening for the GFP fluorescence of progeny. *Tg(-5.1jam1a:CreER<sup>T2</sup>, -5.1jam1a:GFP)<sup>sd34</sup>*: a further 2.9-kb fragment cloned from zebrafish genomic DNA was ligated upstream of both the 2.2-kb promoters (total 5.1 kb). Three *-5.1jam1a:CreER<sup>T2</sup>, -5.1jam1a:GFP* founders were identified by screening for the GFP fluorescence of progeny. *Tg(bactin2:loxP-BFP-loxP-DsRed)<sup>sd27</sup>*: A PCR-amplified *DsRed<sup>l-express</sup>* fragment was used to replace the *EGFP* site in the *pIST2-Myl2-loxP-TagBFP-loxP-EGFP* vector. The *loxP-TagBFP-loxP-DsRed<sup>l-express</sup>* site was then used to replace the *EGFP* site in the *I-SceI-pBSII SK+* vector. A 10.8-kb fragment immediately upstream of the *bactin2* transcriptional start site was cloned from zebrafish genomic DNA and ligated upstream of the *loxP-TagBFP-loxP-DsRed<sup>l-express</sup>* site. Four *bactin2:loxP-BFP-loxP-DsRed* founders were identified by screening for the BFP fluorescence of progeny.

**Cell preparation and flow cytometry.** Kidney marrow cells were prepared as previously described<sup>29</sup>. Briefly, kidneys were dissected, and haematopoietic cells were obtained by macerating the kidney on a stainless steel mesh in 5 ml of ice-cold 2% fetal bovine serum (FBS) in Hanks' balanced salt solution (HBSS). After centrifugation, the pellet was gently mixed with 1 ml of distilled water by pipetting to lyse erythrocytes by osmotic shock. Subsequently, 1 ml of 2× HBSS was added, and the cells were washed with HBSS by centrifugation. Cells from embryos were prepared as previously described<sup>10</sup>. Briefly, embryos were collected and anesthetized in E3 medium containing 0.01% tricaine, and were digested with Liberase TM (Roche, 05401119001) in PBS for 1 h at 37 °C. Cells were then filtered through 40-µm nylon mesh and washed with 2% FBS in HBSS by centrifugation. Just before flow cytometric analysis, Sytox Red (Invitrogen, S34859) solution was added to the samples at a final concentration of 5 nM to exclude nonviable cells. Flow cytometric acquisition was performed on a BD LSR Fortessa (BD Biosciences), and cell sorting was performed on a FACS Aria II (BD Biosciences). Analysis was performed using FlowJo software (Treestar). Cells were sorted into 20% FBS in HBSS, and were used for morphological or expression analysis.

**qPCR and RT-PCR.** Total RNA was extracted from embryos, dissected kidneys, or sorted cells using RNeasy Mini Kit (QIAGEN, 74104), and cDNAs were synthesized using QuantiTect Reverse Transcription Kit (QIAGEN, 205311). Quantitative real-time PCR (qPCR) assays were performed on a BIO-RAD CFX96 real time system according to the manufacturer's instructions (BIO-RAD). The expression of *efla* was used to normalize the amount of the investigated transcripts. Reverse transcription (RT)-PCR was performed as previously described<sup>7</sup>. Primers used in qPCR and RT-PCR are listed in Supplementary Table 2.

**In situ hybridization.** cDNAs were cloned by RT-PCR using specific primers listed in Supplementary Table 2, and ligated into the *pCRII-TOPO* vector (Invitrogen, K4620-01). Digoxigenin (DIG)- or fluorescein-labelled RNA probes were prepared by *in vitro* transcription with linearized constructs as previously described<sup>29</sup>. Embryos were fixed with 4% paraformaldehyde (PFA) in PBS at 4 °C overnight. Whole-mount *in situ* hybridization (WISH) was performed as previously described<sup>30</sup>. Two-colour WISH was performed using DIG- and fluorescein-labelled probes.

Embryos were developed with nitro blue tetrazolium chloride (NBT, Roche, 11383213001)/5-bromo-4-chloro-3-indolyl phosphate, toluidine salt (BCIP, Roche, 11383221001) and FastRed (Roche, 11496549001). Two-colour stained embryos were photographed after removal of the yolk extension tube.

**Immunohistochemistry and haematoxylin and eosin staining.** Embryos were fixed with 4% PFA, embedded in paraffin, and sectioned at 4 µm in thickness. Deparaffinized tissue sections were incubated with blocking solution (1% goat serum, 1% donkey serum, and 0.2% bovine serum albumin in PBS) for 30 min at room temperature and then incubated with 1:1,000 chicken anti-GFP (Aves, GFP-1020), 1:1,000 rabbit anti-RFP antibodies (for DsRed staining, Abcam, ab34771), and/or 1:500 mouse anti-mCherry antibodies (Abcam, ab125096) overnight at 4 °C. For fluorescent immunohistochemistry, sections were incubated with 1:1,000 goat anti-chicken IgG Alexa Fluor 488-conjugated (Molecular Probes, A-11039), 1:1,000 donkey anti-rabbit IgG Alexa Fluor 594-conjugated (Molecular Probes, A-21207), and/or goat anti-mouse IgG Alexa Fluor 594-conjugated (Molecular Probes, A-11005) secondary antibodies for 1 h at room temperature. After washing, sections were mounted with Duolink *in situ* mounting medium with DAPI (Olink, DUO82040). For colometric immunohistochemistry, sections were stained with anti-GFP antibody, followed by staining with 1:1,000 anti-chicken IgG horseradish peroxidase (HRP)-conjugated secondary antibody (Invitrogen, 61-3120) for 1 h at room temperature. Sections were then developed with 3, 3'-diaminobenzidine (DAB) substrate solution (Sigma, D5905) for 3 min at room temperature. After washing, sections were mounted with mounting medium (50% glycerol, 10% gelatin in double-distilled H<sub>2</sub>O). Whole-mount immunofluorescence was performed as described<sup>4</sup>, using 1:500 mouse anti-cMyc antibody (Sigma, M4439) and 1:1,000 donkey anti-mouse IgG Alexa Fluor 488-conjugated (Molecular Probes, A-21202). Haematoxylin and eosin staining was performed on deparaffinized tissue sections as previously described<sup>29</sup>.

**Transient expression.** A *Flag* and *HA* tag were inserted between the two Ig domains of *jam1a* and *jam2a* by two-step PCR, respectively, and cloned into the *pcDNA3* vector as previously described<sup>29</sup>. HEK293T or HeLa cells were transiently transfected with the above constructs using FuGENE HD transfection reagent (Promega, E2311). Cells were then cultured in six-well plate with 10% FBS, 200 mM L-glutamine in Dulbecco's modified Eagle medium (DMEM) at 37 °C and 5% CO<sub>2</sub>.

**Immunoprecipitation and western blotting.** HEK293T cells expressing *Jam1a-Flag* and/or *Jam2a-HA* constructs were harvested and lysed in lysis buffer (25 mM Tris-HCl pH 7.4, 1 mM EDTA, 0.1 mM EGTA, 150 mM NaCl, 5 mM MgCl<sub>2</sub>, 2 mM Na<sub>3</sub>VO<sub>4</sub>, 20% glycerol, 0.1% Triton X-100, 1 mM dithiothreitol, proteinase inhibitor). Samples were then centrifuged to remove precipitated proteins and incubated with anti-Flag M2 agarose antibody (Sigma, A2220) for 3 h at 4 °C. Samples were washed three times with lysis buffer, resuspended in 2× sample buffer (4% SDS, 0.2 M dithiothreitol, 0.1 M Tris-HCl pH 6.8, 10% glycerol, 20 µg ml<sup>-1</sup> bromophenol blue), and boiled for loading. Western blotting was performed as previously described<sup>31</sup>. Briefly, samples were separated by a NuPAGE 4–12% Bis-Tris Gel (Novax, NP0335BOX). The gel was then transferred using Semi-Dry transfer cell (BIO-RAD) to Immobilon-P Membrane (Millipore, IPVH00010). The membrane was blocked with 1% skim milk, 0.05% Tween-20 in PBS for 30 min at room temperature, and then incubated with 1:1,000 mouse anti-HA antibody (Covance, MMS-101P) or 1:1,000 rabbit anti-Flag antibody (Sigma, F7425) overnight at 4 °C. After washing with 0.05% Tween-20 in PBS (PBST), the membrane was incubated with 1:10,000 goat anti-mouse IgG HRP-conjugated secondary antibody (Jackson ImmunoResearch, 115-035-166) or 1:10,000 goat anti-rabbit IgG HRP-conjugated secondary antibody (Jackson ImmunoResearch, 111-035-144) for 45 min at room temperature. After washing with PBST, chemiluminescence was performed using the SuperSignal West Pico Chemiluminescent Substrate (Thermo, 34077).

**Duolink proximity ligation assay.** HeLa cells expressing *Jam1a-Flag* or *Jam2a-HA* construct were co-cultured on a cover slip. Cells were fixed with 4% PFA for 20 min at room temperature, blocked with 0.1% gelatin-PBS, and stained with 1:1,000 rabbit anti-Flag and 1:1,000 mouse anti-HA antibodies for 40 min at room temperature. After washing with 0.1% gelatin-PBS, proximity ligation assay (PLA) was done according to manufacturer's protocol (Olink). Cells were then stained with 1:1,000 donkey anti-mouse IgG Alexa Fluor 488-conjugated and 1:1,000 goat anti-rabbit IgG Alexa Fluor 647-conjugated (Molecular Probes, A-21244) secondary antibodies for 40 min at room temperature. After washing with 0.1% gelatin-PBS, cells were mounted with Duolink *in situ* mounting medium with DAPI.

**Microscopy and acridine orange staining.** Fluorescent images were captured using an SP5 inverted confocal microscope (Leica) as previously described<sup>10</sup>. For time-lapse imaging, embryos were embedded in agarose (1.0% in E3 medium) containing tricaine at a temperature of 28.5 °C. *z*-stacks were taken every 196 s. Videos were created following processing with Velocity software (Improvision). Acridine orange staining was performed as previously described<sup>32</sup>. Briefly, embryos were dechorionated and incubated in 1× E3 medium containing 5 µg ml<sup>-1</sup> acridine orange (Sigma, A8097) for 30 min, followed by three washes in 1× E3. Embryos were then visualized by confocal microscopy. All images captured by confocal microscopy

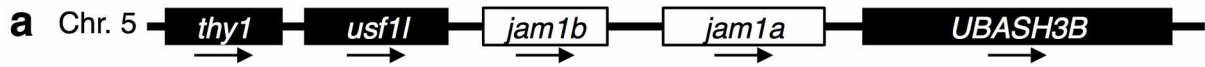
were displayed as maximum projections. Visible light imaging was performed on a BX-51 microscope using 100× oil objective lens and DP70 digital camera and software (Olympus) or a Leica MZ16 microscope and DFC295 digital camera and software (Leica).

**Morpholino and mRNA injection.** Embryos were injected at the one-cell stage with 1 nl of morpholino oligonucleotides (MOs, GeneTools) and/or mRNA. The MO sequences and concentrations used in this study are as follows: *jam1a* MOatg, AGCACACAAAGGCGAAGGTCAACAT (100 μM); *jam1a* MO control, AGgAg ACAAAcGCcAAGcTCAACAT (100 μM, lowercase letters denote mismatched bases); *jam1a* MOex7, ATCACCTTTAACAGAGAACAACACA (300 μM); *jam2a* MOex5, AGGAACTACAGCAGAAACAGGTCAA (400 μM). The *jam2a* MOatg (300 μM)<sup>15</sup> and *wnt16* MO2 (5ng/nl)<sup>4</sup> were used as previously reported. The effects of MOs are summarized in Supplementary Table 1. Capped mRNAs were synthesized from linearized pCS2+ constructs using the mMessage mMachine SP6 kit (Ambion, AM1340), and were injected into embryos at following concentrations; *dlc*, 50 ng μl<sup>-1</sup>; *dld*, 50 ng μl<sup>-1</sup>.

**4OHT treatment.** 4-hydroxytamoxifen (4OHT, Sigma, H7904) was dissolved in ethanol as a 25 mM stock solution. Embryos were incubated with 5 μM of 4OHT in E3 medium. Control embryos were incubated in E3 medium containing 0.02% ethanol. After treatment, the embryos were washed twice in E3 medium and grown as described above.

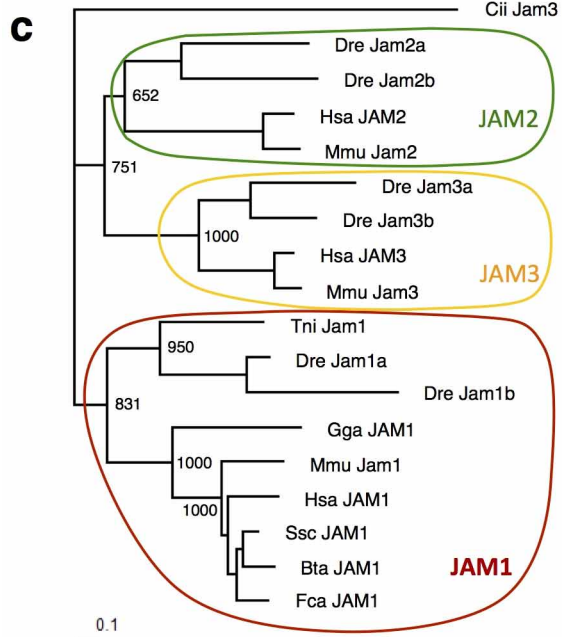
**Experimental design and statistics.** All experiments comparing treatment groups were made using randomly assigned siblings without investigator blinding. Sample sizes were chosen after estimating effect size, and data were analysed for statistical significance after at least two repeated experiments. All data were analysed by comparison of means using unpaired two-tailed Student's *t*-tests. No data were excluded. A value of *P* < 0.01 was considered to be statistically significant.

21. Westerfield, M. *The Zebrafish Book: a Guide for the Laboratory Use of Zebrafish* (Danio rerio) (Univ. Oregon Press, 2000).
22. North, T. E. *et al.* Prostaglandin E2 regulates vertebrate haematopoietic stem cell homeostasis. *Nature* **447**, 1007–1011 (2007).
23. Chi, N. C. *et al.* Foxn4 directly regulates *tbx2b* expression and atrioventricular canal formation. *Genes Dev.* **22**, 734–739 (2008).
24. Lawson, N. D. & Weinstein, B. M. *In vivo* imaging of embryonic vascular development using transgenic zebrafish. *Dev. Biol.* **248**, 307–318 (2002).
25. Villefranc, J. A., Amigo, J. & Lawson, N. D. Gateway compatible vectors for analysis of gene function in the zebrafish. *Dev. Dyn.* **236**, 3077–3087 (2007).
26. Distel, M., Wullmann, M. F. & Koster, R. W. Optimized Gal4 genetics for permanent gene expression mapping in zebrafish. *Proc. Natl Acad. Sci. USA* **106**, 13365–13370 (2009).
27. Higashijima, S., Okamoto, H., Ueno, N., Hotta, Y. & Eguchi, G. High-frequency generation of transgenic zebrafish which reliably express GFP in whole muscles or the whole body by using promoters of zebrafish origin. *Dev. Biol.* **192**, 289–299 (1997).
28. Zygmunt, T. *et al.* Semaphorin-PlexinD1 signaling limits angiogenic potential via the VEGF decoy receptor sFlt1. *Dev. Cell* **21**, 301–314 (2011).
29. Kobayashi, I. *et al.* Characterization and localization of side population (SP) cells in zebrafish kidney hematopoietic tissue. *Blood* **111**, 1131–1137 (2008).
30. Thisse, C., Thisse, B., Schilling, T. F. & Postlethwait, J. H. Structure of the zebrafish *snail1* gene and its expression in wild-type, *spadetail* and *no tail* mutant embryos. *Development* **119**, 1203–1215 (1993).
31. Fujita, N. *et al.* The Atg16L complex specifies the site of LC3 lipidation for membrane biogenesis in autophagy. *Mol. Biol. Cell* **19**, 2092–2100 (2008).
32. Furutani-Seiki, M. *et al.* Neural degeneration mutants in the zebrafish, *Danio rerio*. *Development* **123**, 229–239 (1996).

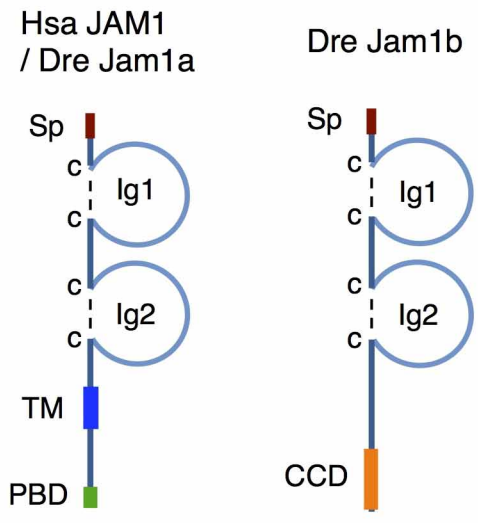


**b**

Hsa JAM1	MGTKAQVERKLLCLFILAILLCSLALG	SVTVHSSEPEVRIPENNPVKLS	CAYSGFS--SPRVEWKF	DQGD-TTRLVCYNN
Dre Jam1a	-----MLTFAFVCFSLFVTGIHG	FQVTVTS--PVKVENEGVDLQ	CSYTSDFGATPRVEWKF	KDLKGSQTLVYFDG
Dre Jam1b	-----MLTLVFVCLSFSLTGLH	ASFVAVNGPIVKVENEGVDLQ	CSYTADFGATPRVEWKF	RNLKGFQYFIYFNN
	* * :	: . .	:: ** : * . * : .	: * * * * * : . : : .
Hsa JAM1	KITASIEDRVTLFPTGITFKSV	TREDTGYTCMVSEEGGNSY	GEVVKVLIVLPPSKPTVNI	PSSATIGNRAVLTCSEQD
Dre Jam1a	KPTGQYTGRTVMYDKGLRFNK	VTRADTDGIDCEVSGSGG--	YGENTIKLTVLPPAKPVSR	IPSSVTSSNVRLTCFDPV
Dre Jam1b	KPTVEYEQRITVYAGGLRFQ	KVTRADAGDYNCEVSGNGG--	YGENTIKLVVSVPPSKPV	SSIPSSVTGGSNVRLTCFDPV
	* * . * * :	* : * . * * * * * * * *	* * * * * . * * * * * * * *	* * * * * * * * * * * * * *
Hsa JAM1	GSPPEYTWFKDGI	VMPNPKSTRAFSNSSY	VLNPTTGELVFDPLS	ASDTGEYSC
Dre Jam1a	GSPPEYTWFKDGI	VMPNPKSTRAFSNSSY	VLNPTTGELVFDPLS	ASDTGEYSC
Dre Jam1b	GSPPEYTWFKDGI	VMPNPKSTRAFSNSSY	VLNPTTGELVFDPLS	ASDTGEYSC
	* * * * * * * * * * * * * *	* * * * * * * * * * * * * *	* * * * * * * * * * * * * *	* * * * * * * * * * * * * *
Hsa JAM1	VIVA	AVLVTLILLGILVFGIWFAY	SRGHFDRTKKGTSSK	KVIYSQPS---ARSEGEFK
Dre Jam1a	GIVAGVIVALLAVGLL	FGLWYASKKG	YLPKLSETKQKQAVYT	QPQTDDVDEANGFRQKS
Dre Jam1b	QVLDVKS	NLSMETHNIPGKITNSH	IMEKQYGVFMLEQEV	KLKLEIQKLELEVTKL
	: : : : : : : : : : : :	: : : : : : : : : : : :	: : : : : : : : : : : *	: : : : : : : : : : : * . . . *



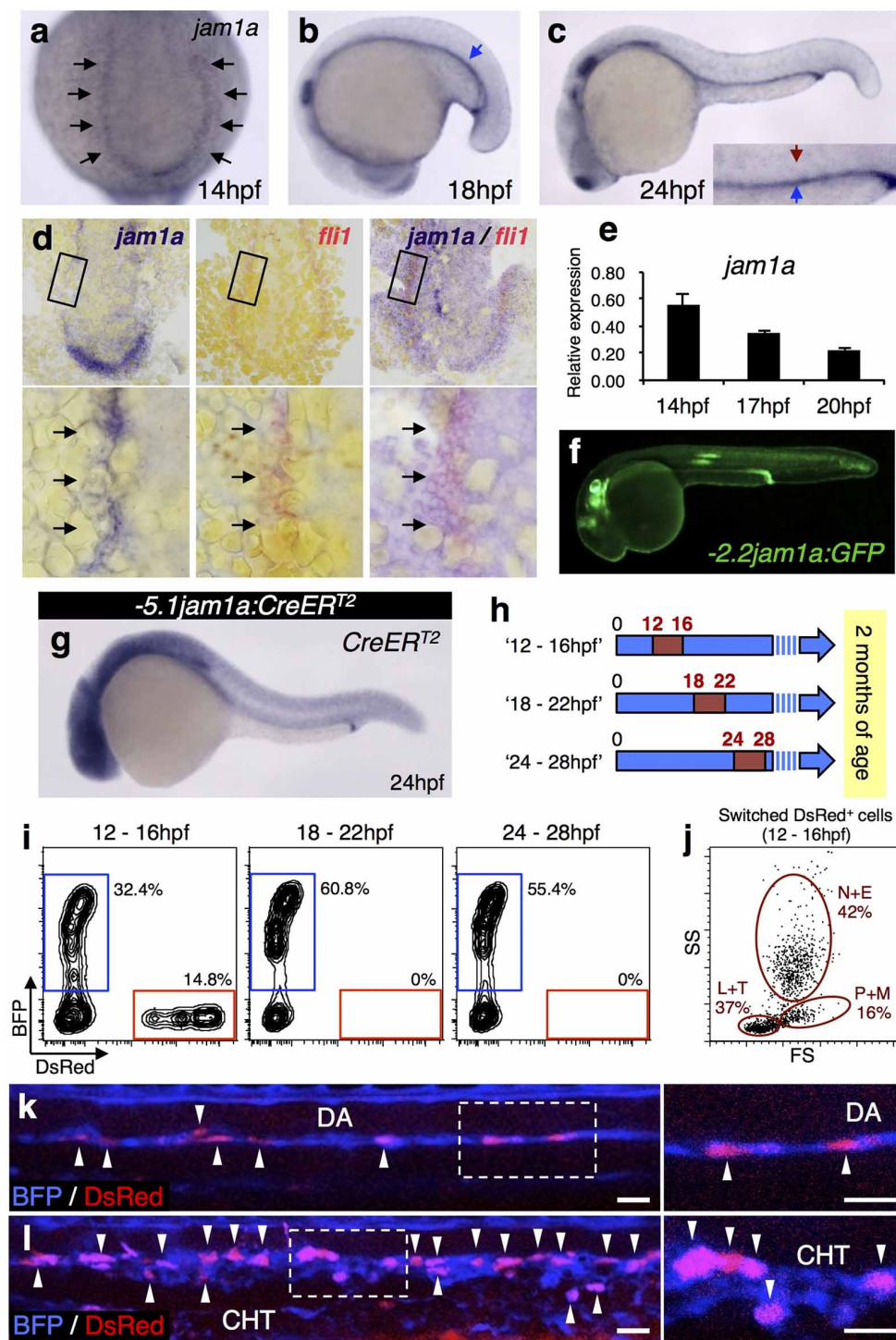
**d**



**Extended Data Figure 1 | Alignment and phylogenetic analysis of Jam1a.**

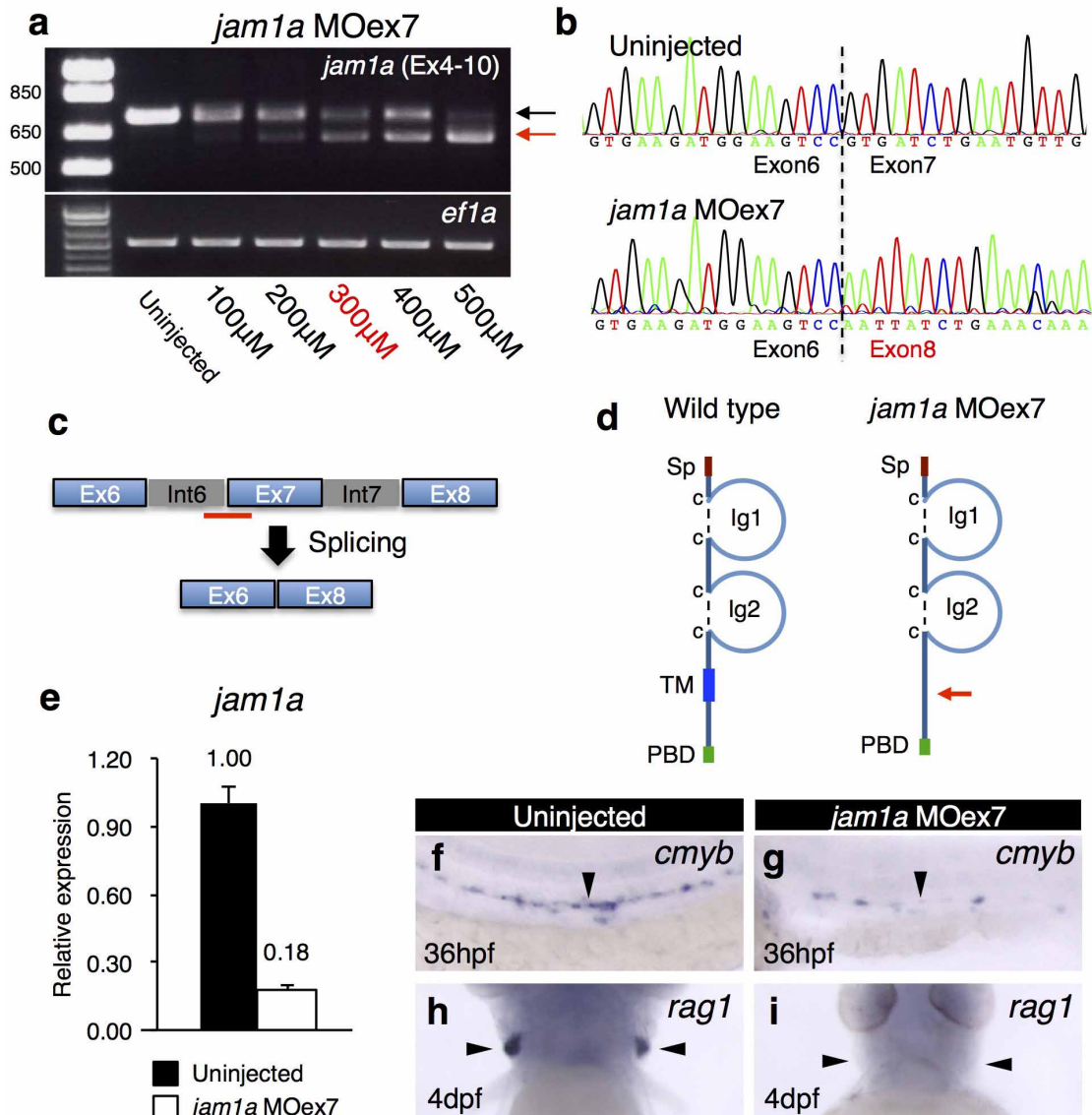
**a**, The genomic loci of the *jam1a* and *jam1b* genes. Arrows indicate the orientation of each gene. **b**, Alignment of zebrafish Jam1a, Jam1b, and human JAM1. The multiple alignment was produced using ClustalW. Asterisks indicate a fully conserved residue. Colons and periods indicate strong and weak similarity, respectively. Dashes indicate gaps. Boxes coloured red, signal peptide (Sp); light blue, immunoglobulin-like domain (Ig); blue, transmembrane domain (TM); green, PDZ-binding domain (PBD); yellow, coiled-coil domain

(CCD). Shaded boxes show a cis-dimerization motif. **c**, Phylogenetic analysis of Jam proteins. Cii, *Ciona intestinalis*; Dre, *Danio rerio*; Hsa, *Homo sapiens*; Mmu, *Mus musculus*; Tni, *Tetraodon nigroviridis*; Gga, *Gallus gallus*; Ssc, *Sus scrofa*; Bta, *Bos taurus*; Fca, *Felis silvestris catus*. Cii Jam3 was used as an out-group. The numbers at the relevant branches refer to bootstrap values of 1,000 replications. **d**, Schematic diagrams of human JAM1 and zebrafish Jam1a (left) and Jam1b (right).



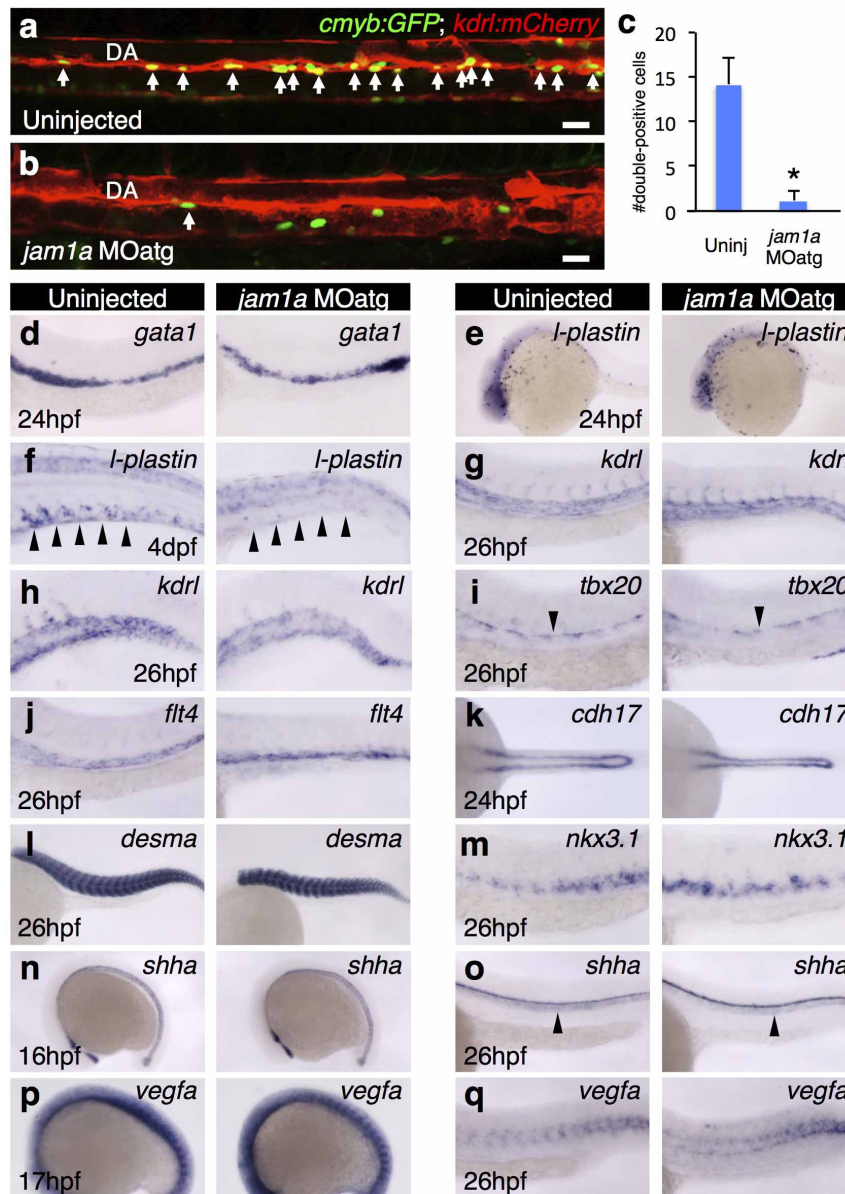
**Extended Data Figure 2 | The expression of *jam1a* and lineage tracing of *jam1a*-expressing cells.** **a–c**, The expression of *jam1a* at 14, 18 and 24 hpf. Black, blue, and red arrows indicate the posterior lateral mesoderm (PLM), pronephros, and dorsal aorta (DA), respectively. **d**, Single or two-colour whole-mount *in situ* hybridization with *jam1a* (purple) and/or *fli1* (red) probes. The expression domain of *fli1* merged with that of *jam1a* (arrows). **e**, qPCR analysis of *jam1a* in purified *fli1*:GFP<sup>+</sup> cells at 14, 17, and 20 hpf. Relative expression levels in each cell population were calculated from the expression levels in the kidney tissue. Error bars, s.d. **f**, GFP expression of -2.2*jam1a*:GFP at 30 hpf. GFP expression was strongly detected in posterior pronephros, lateral lines, and otic vesicles. **g**, The expression of CreER<sup>T2</sup> in -5.1*jam1a*:CreER<sup>T2</sup> at 24 hpf. **h**, Three different schedules of 4-hydroxytamoxifen (4OHT) treatment (12–16 hpf, 18–22 hpf, and 24–28 hpf) in -5.1*jam1a*:CreER<sup>T2</sup>; *bactin2*:loxP-BFP-loxP-DsRed. The numbers indicate hour post fertilization (hpf), and red insets

in the blue arrows indicate the period of the 4OHT treatment. **i**, Flow cytometric analysis of kidney marrow cells in 12–16 hpf group (left,  $n = 5$ ), 18–22 hpf group (middle,  $n = 5$ ), and 24–28 hpf group (right,  $n = 2$ ) at 2 months of age. One 12–16 hpf animal showed switched DsRed<sup>+</sup> cells in kidney marrow cells. **j**, DsRed<sup>+</sup> cells from 12–16 hpf kidneys are distributed in all blood cell populations, including neutrophils and eosinophils (N+E), precursors and monocytes (P+M), and lymphocytes and thrombocytes (L+T). **k, l**, Confocal imaging of the DA and caudal haematopoietic tissue (CHT) in a 12–16 hpf embryo at 48 hpf. Right panels show high magnification views of the boxed regions in left panels. Embryos are oriented with anterior to the left. There are many ‘switched’ DsRed<sup>+</sup> cells in the ventral floor of the DA and in the CHT (arrowheads). Bars, 20  $\mu$ m. Data are representative of two independent experiments with two different clutches of embryos (**a–e, g**) or eight embryos (**k, l**) or pooled from two independent experiments (**i, j**).



**Extended Data Figure 3 | Characterization of *jam1a* MOex7-injected embryos.** **a**, RT-PCR results from *jam1a* MOex7-injected embryos. cDNA from embryos uninjected or injected with various doses of *jam1a* MOex7 (100–500  $\mu$ M) was subjected to RT-PCR analysis using specific primers, which amplify from exon 4 to 10 of *jam1a*. *ef1a* was used as a control. The expected size of PCR products in uninjected embryos is 746 base pairs (bp) (black arrow). Exon 7 (108 bp)-skipped products were detected in *jam1a* MOex7-injected embryos (red arrow). The dose of 300  $\mu$ M was used in this study. **b**, Exon 7-skipped products were verified by sequencing. The dotted line indicates the junctions between exon 6 and exon 7 (uninjected, upper panel) or exon 8 (*jam1a* MOex7, lower panel). **c**, A schematic diagram of the mRNA splicing in *jam1a* MOex7-injected embryos. The red bar indicates the binding site of

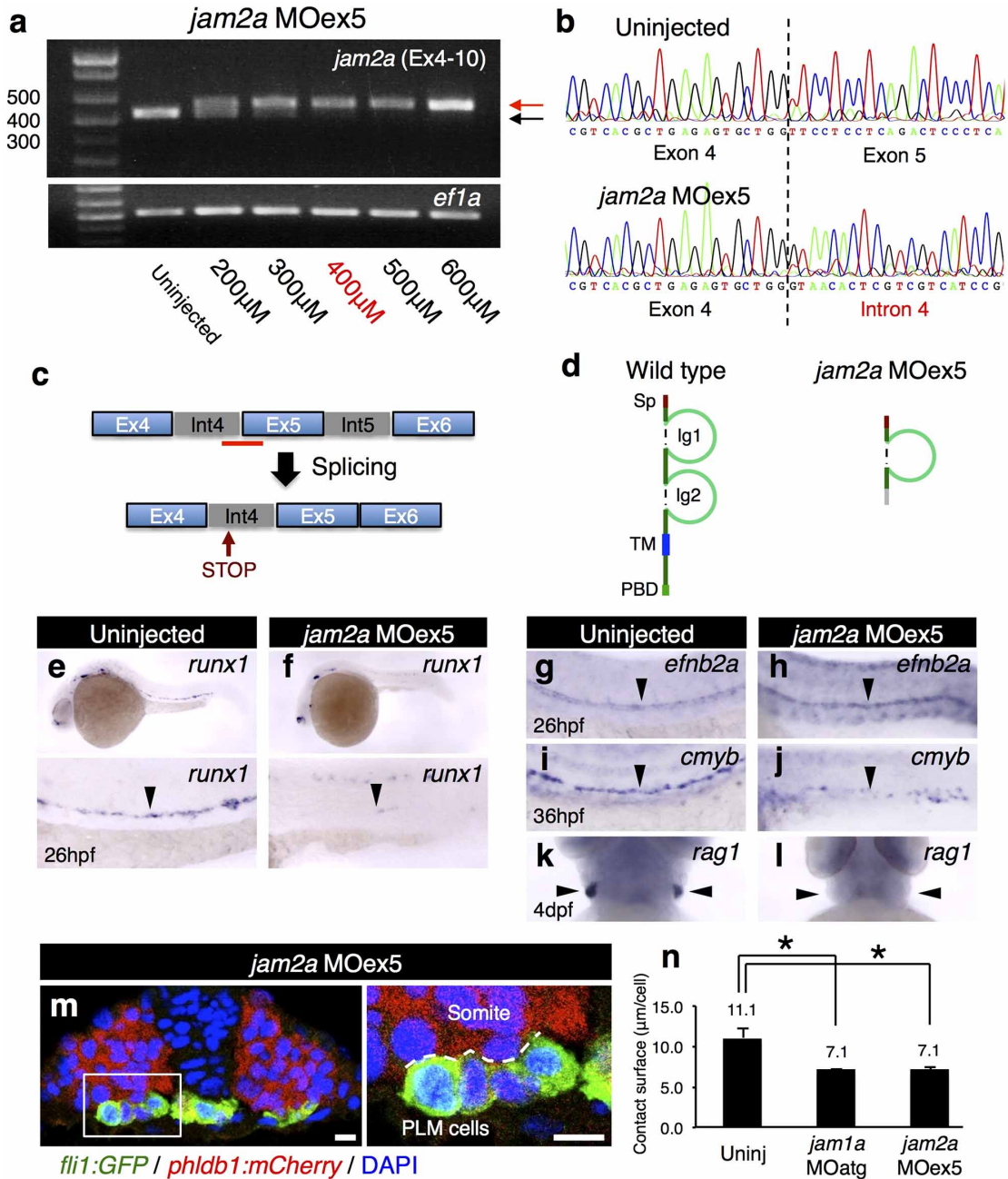
*jam1a* MOex7. **d**, Schematic diagrams of Jam1a protein in wild-type (left) or *jam1a* MOex7-injected embryos (right). Since exon 7 encodes the transmembrane domain (TM), *jam1a* MOex7-injected embryos express a mutant protein lacking the TM. Sp, signal peptide; Ig, immunoglobulin-like domain; PBD, PDZ-binding domain. **e**, The relative expression of wild-type *jam1a* mRNA in uninjected or *jam1a* MOex7 (300  $\mu$ M)-injected embryos at 24 hpf. The reverse primer was designed in exon 7. Error bars, s.d. **f–i**, The expression of *cmyb* and *rag1* in uninjected or *jam1a* MOex7-injected embryos. Arrowheads indicate the dorsal aorta (**f, g**) or the thymus (**h, i**). Data are representative of two independent experiments with two different clutches of embryos (**a, e–i**).



#### Extended Data Figure 4 | *jam1a* is required for HSC specification.

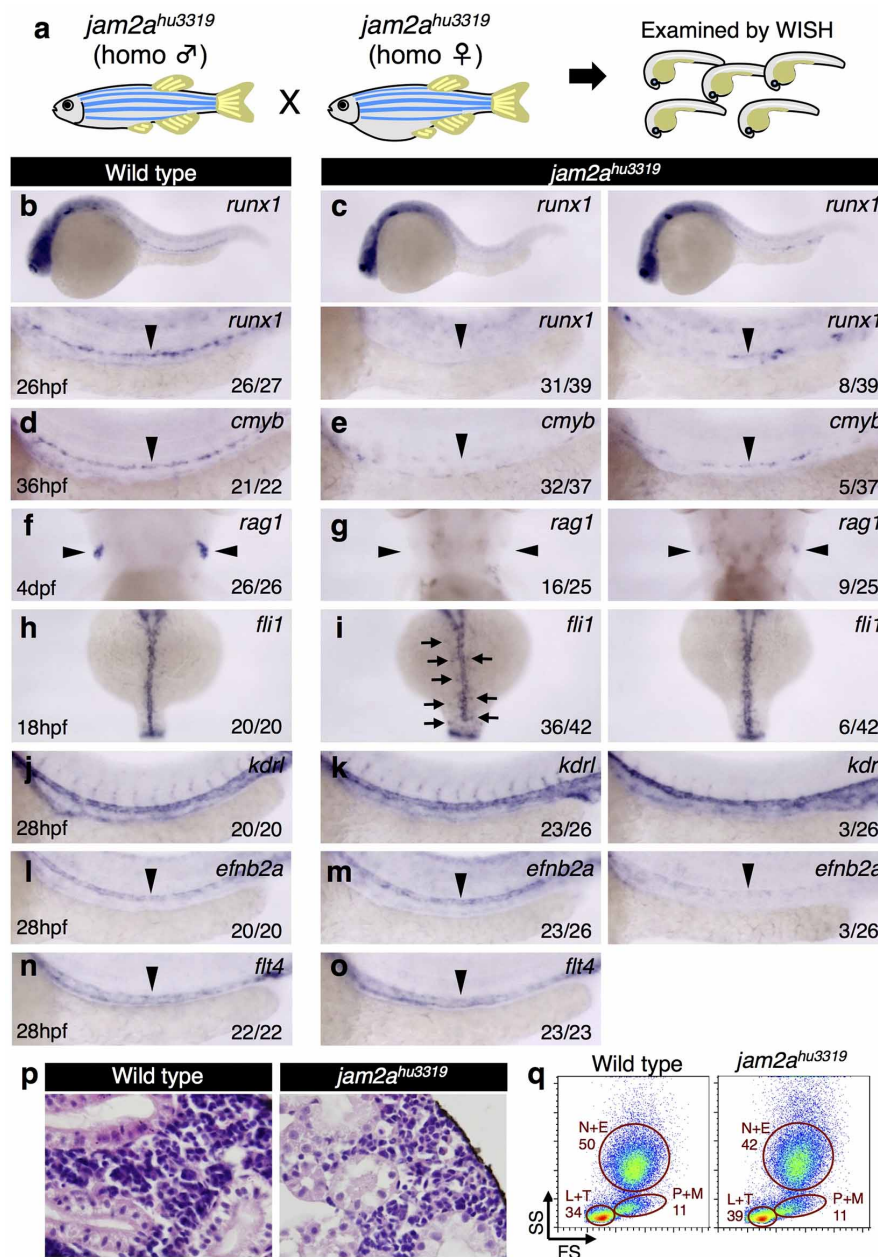
**a–c**, Fluorescently labelled HSCs in *cmyb:GFP; kdrl:mCherry*. The number of *cmyb:GFP; kdrl:mCherry* double-positive cells in the dorsal aorta (DA) were counted in uninjected or *jam1a* MOatg-injected embryos at 48 hpf (arrows). Embryos are oriented with anterior to the left. The average number of double-positive cells is significantly lower in *jam1a* MOatg-injected embryos ( $n = 10$ ) compared with uninjected embryos ( $n = 10$ ),  $*P < 0.001$  by Student's *t*-test; error bars, s. d. **d–q**, The expression of *gata1* (an erythroid marker), *l-plastin* (a

myeloid marker) at 24 hpf or 4 dpf, *kdrl* (a pan-endothelial marker) in the trunk or caudal haematopoietic tissue (CHT), *tbx20* (a marker for the roof of DA), *flt4* (a vein marker), *cdh17* (a pronephros marker), *desma* (a somite marker), *nkx3.1* (a sclerotome marker), *shha* (a notochord marker) at 16 hpf or 26 hpf, and *vegfa* at 17 hpf or 26 hpf in uninjected or *jam1a* MOatg-injected embryos. Arrowheads indicate CHT (**f**), DA (**i**), or notochord (**o**). Data are representative of two independent experiments with ten embryos (**a–c**) or two different clutches of embryos (**d–q**).



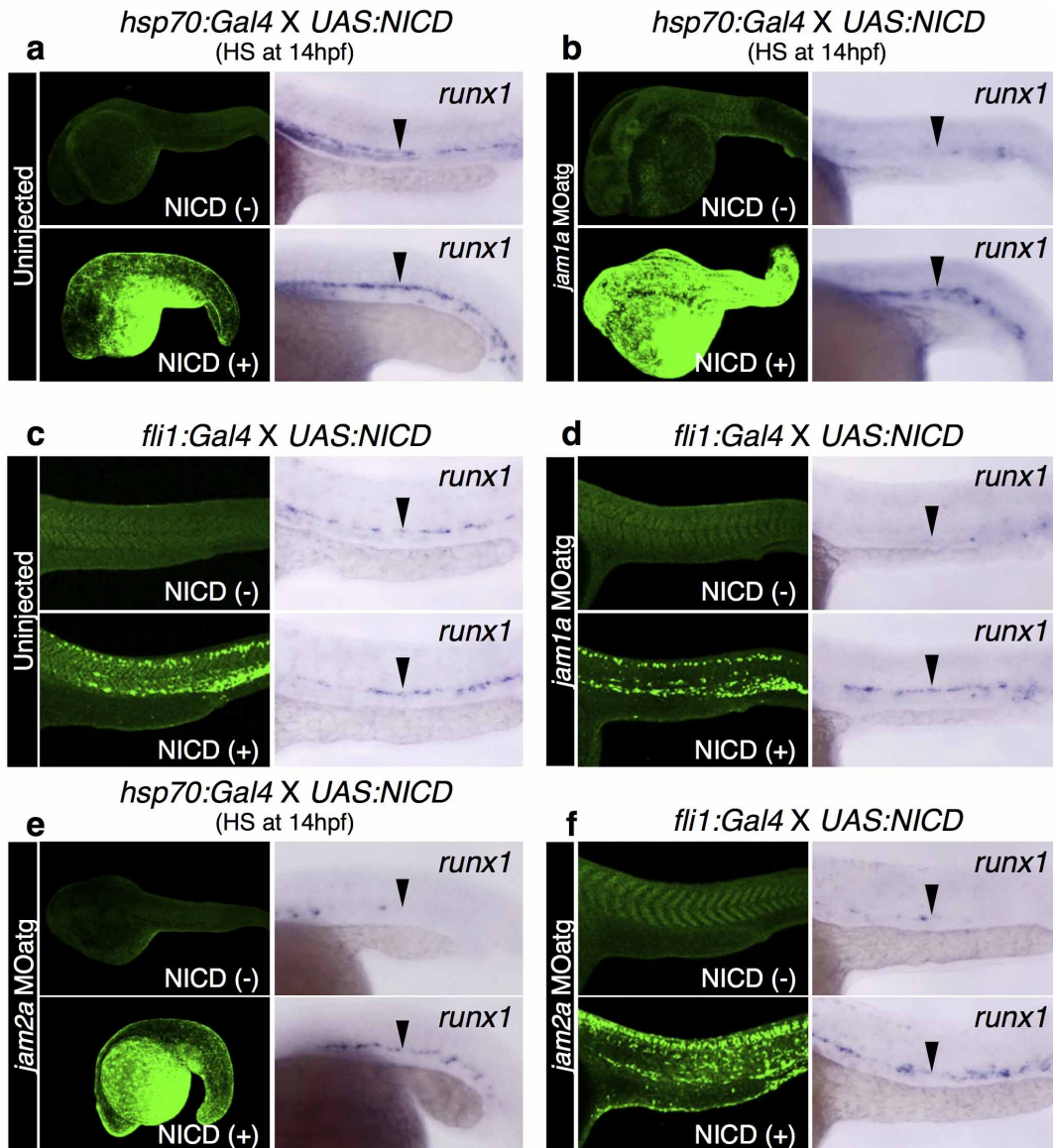
**Extended Data Figure 5 | Characterization of *jam2a* MOex5-injected embryos.** **a**, RT-PCR results from *jam2a* MOex5-injected embryos. cDNA from embryos uninjected or injected with various doses of *jam2a* MOex5 (200–600  $\mu$ M) was subjected to RT-PCR analysis using specific primers, which amplify from exon 4 to 10 of *jam2a*. *ef1a* was used as a control. The expected size of PCR products in uninjected embryos is 537 base pairs (bp) (black arrow). Intron 4 (72 bp)-trapped products were detected in *jam2a* MOex5-injected embryos (red arrow). The dose of 400  $\mu$ M was used in this study. **b**, Intron 4-trapped products were verified by sequencing. The dotted line indicates the junctions between exon 4 and exon 5 (uninjected, upper panel) or intron 4 (*jam2a* MOex5, lower panel). **c**, A schematic diagram of the mRNA splicing in *jam2a* MOex5-injected embryos. The red bar indicates the binding site of *jam2a* MOex5. **d**, Schematic diagrams of Jam2a protein in wild-type (left) or *jam2a* MOex5-injected embryos (right). Since intron 4 contains an in-frame stop codon, *jam2a* MOex5-injected embryos express a truncated mutant

protein. Sp, signal peptide; Ig, immunoglobulin-like domain; TM, transmembrane domain; PBD, PDZ-binding domain. **e–l**, The expression of *runx1*, *efnb2a*, *cmyb*, and *rag1* in uninjected or *jam2a* MOex5-injected embryos. Arrowheads indicate the dorsal aorta (**e–j**) or the thymus (**k, l**). **m**, A transverse section of a *fli1*:GFP; *phldb1*:mCherry embryo injected with *jam2a* MOex5 at 16 hpf. A high magnification view of the boxed region is shown in the right panel. A dotted line in the right panel indicates the contact surface area between *fli1*:GFP<sup>+</sup> PLM cells and *phldb1*:mCherry<sup>+</sup> somitic cells. Bars, 10  $\mu$ m. **n**, The average contact surface area between a PLM cell and the somite in uninjected, *jam1a* MOatg-, or *jam2a* MOex5-injected embryos. The contact surface area per cell ( $\mu$ m per cell) was calculated from at least one hundred *fli1*:GFP<sup>+</sup> cells in an embryo, and the averages were obtained from three embryos of each. \* $P < 0.01$ , by Student's *t*-test. Error bars, s.d. Data are representative of two independent experiments with two different clutches of embryos (**a, e–l**) or three embryos (**m, n**).



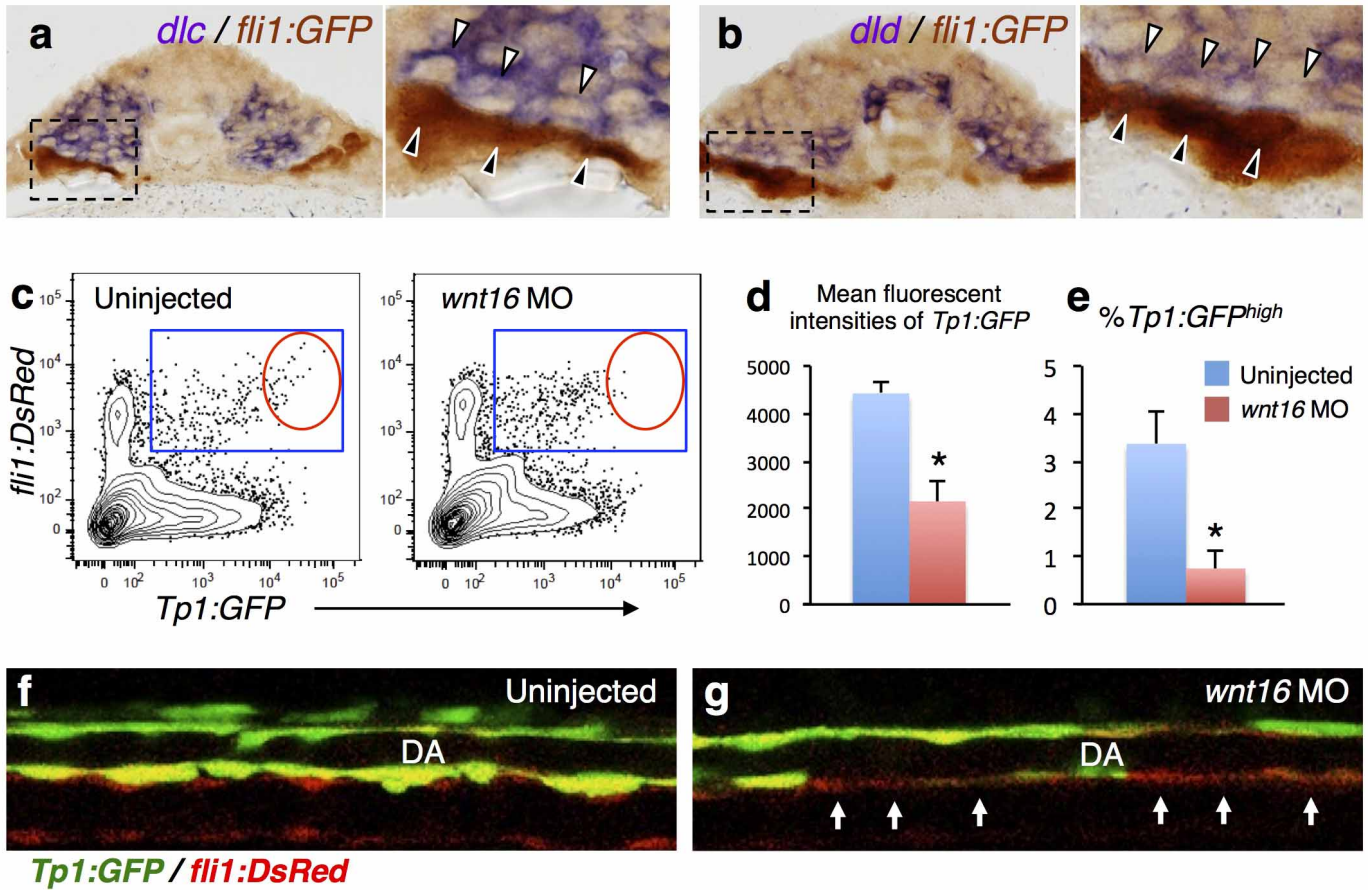
**Extended Data Figure 6 | *jam2a* is required for HSC specification.** **a**, A schematic diagram of the preparation of *jam2a* mutant (*jam2a*<sup>hu3319</sup>) embryos. Embryos from an incross of genotyped homozygous (homo) *jam2a*<sup>hu3319</sup> animals were examined by whole-mount *in situ* hybridization (WISH). **b–g**, The expression of *runx1* and *cmyb* in the dorsal aorta (DA) and *rag1* in the thymus in wild-type or *jam2a*<sup>hu3319</sup> embryos. The numbers shown in each panel indicate the frequency of embryos showing each expression pattern. **h, i**, The expression of *fli1* at 18 hpf in wild-type or *jam2a*<sup>hu3319</sup> embryos. Arrows indicate a subset of *fli1*<sup>+</sup> cells that did not reach the midline. **j–o**, The expression of endothelial marker genes (*kdrl*, *efnb2a*, and *flt4*) in wild-type or *jam2a*<sup>hu3319</sup> embryos at 28 hpf. Approximately 90% of embryos showed normal

vascular plexus, while the rest of embryos showed a reduction of *efnb2a* and *kdrl*. Arrowheads indicate the DA (**b–e, l, m**), the thymus (**f, g**), or posterior cardinal vein (**n, o**). **p**, Histological analysis of the adult kidney in a wild-type or *jam2a*<sup>hu3319</sup> animal at 2 months of age. Many blood cells are observed in the marrow area. Haematoxylin and eosin (HE) staining. **q**, Representative results of flow cytometric analysis of kidney marrow cells from a wild-type or *jam2a*<sup>hu3319</sup> animal at 3 months of age. All blood cell populations are detected in *jam2a*<sup>hu3319</sup> animals. L+T, lymphocytes and thrombocytes; N+E, neutrophils and eosinophils; P+M, precursors and monocytes. Data are representative of two independent experiments with two different clutches of embryos (**b–o**) or three different animals (**p, q**).



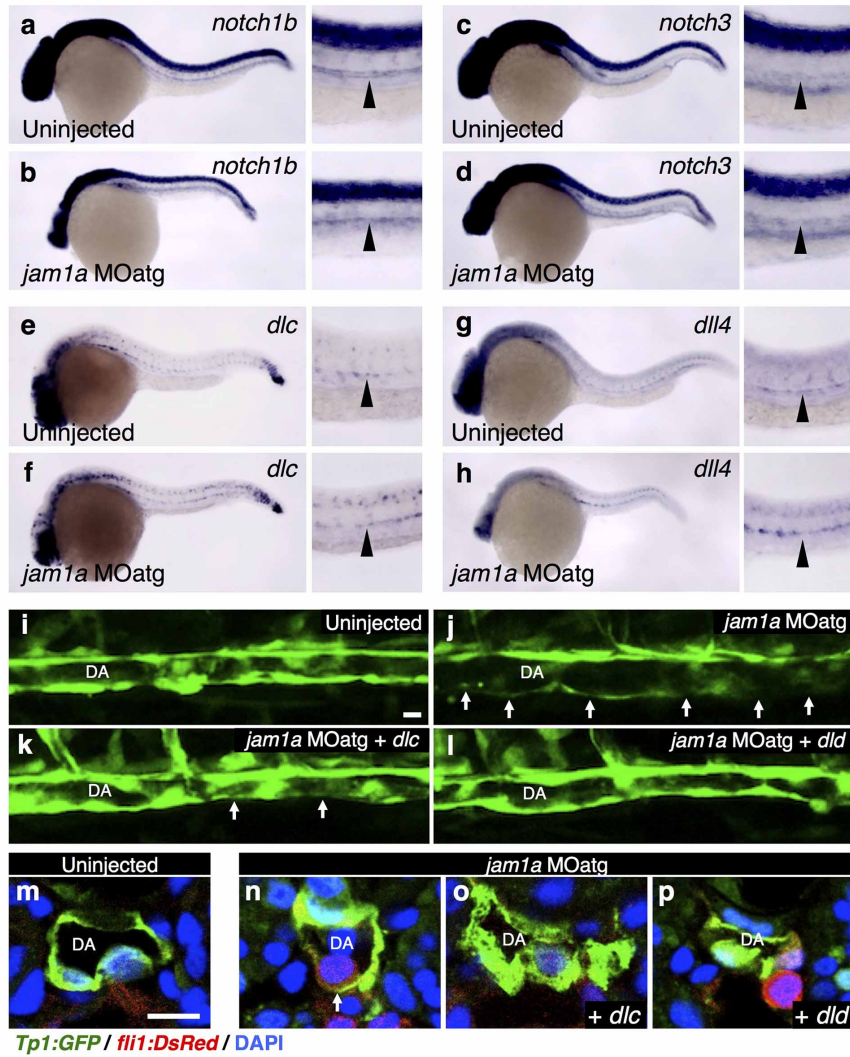
**Extended Data Figure 7 | Enforced expression of the Notch intracellular domain rescues HSCs in *jam1a* or *jam2a* morphants.** Heat-shock (HS) (*hsp70:Gal4*, **a**, **b**, **e**) or endothelial (*fli1:Gal4*, **c**, **d**, **f**) induction of Notch intracellular domain (NICD) in uninjected, *jam1a* MOatg-, or *jam2a* MOatg-injected embryos. Left panels show whole-mount immunofluorescence

visualization of Myc-tagged NICD, and right panels show the expression of *runx1* at 26 hpf. Arrowheads indicate the dorsal aorta. Data are representative of two independent experiments with two different clutches of embryos (**a**–**f**).



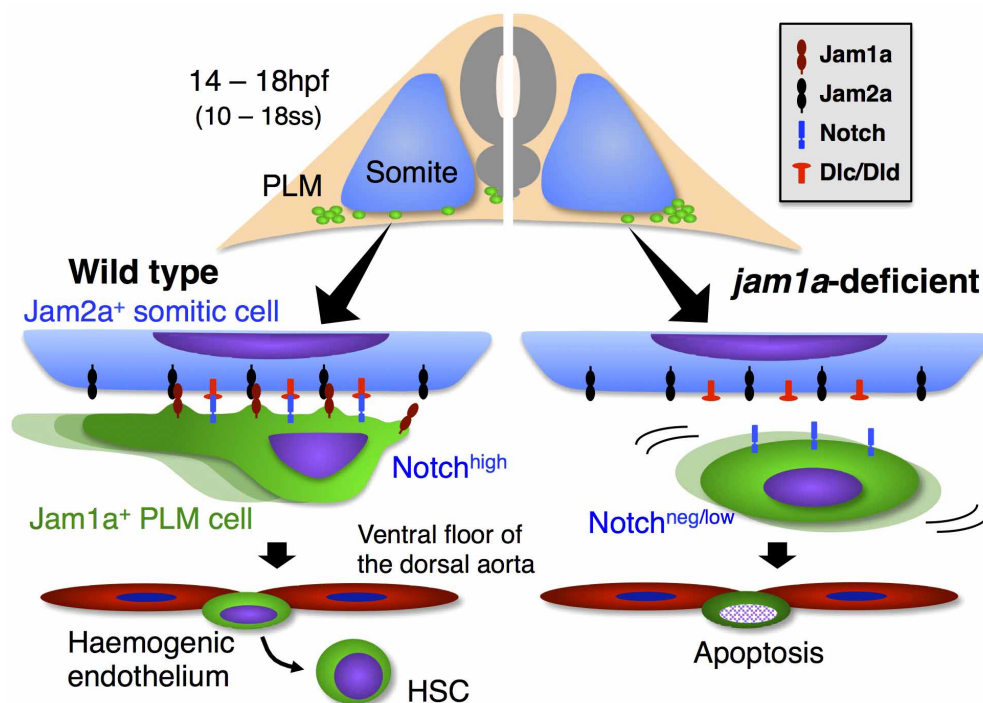
**Extended Data Figure 8 | Somitic Dlc and Dld are involved in the activation of endothelial Notch signalling.** **a, b**, Transverse sections of *fli1:GFP* embryos stained with *dlc* or *dld* (purple) and anti-GFP antibody (brown) at 15 hpf. Right panels show high magnification views of the boxed regions. Migrating *fli1:GFP*<sup>+</sup> cells (black arrowheads) are in contact with *dlc*<sup>+</sup> or *dld*<sup>+</sup> somitic cells (white arrowheads). **c–e**, Flow cytometric analysis of *Tp1:GFP*; *fli1:DsRed* embryos uninjected or injected with *wnt16* MO at 22 hpf. Representative results of flow cytometric analysis (**c**), the mean fluorescent intensities of GFP in *Tp1:GFP*<sup>+</sup>; *fli1:DsRed*<sup>+</sup> populations (**d**), and the percentages of *Tp1:GFP*<sup>high</sup> in

*fli1:DsRed*<sup>+</sup> populations (**e**) are shown. Blue gates and red circles indicate the *Tp1:GFP*<sup>+</sup>; *fli1:DsRed*<sup>+</sup> and *Tp1:GFP*<sup>high</sup>; *fli1:DsRed*<sup>+</sup> population, respectively. \**P* < 0.01, by Student's *t*-test. Error bars, s.d. **f, g**, Lateral views of the dorsal aorta (DA) in *Tp1:GFP*; *fli1:DsRed* embryos uninjected or injected with *wnt16* MO at 28 hpf. Arrows indicate the low activation of *Tp1:GFP* in the ventral floor of the DA. Data are representative of two independent experiments with four embryos (**a, b**), eight embryos (**f, g**), or four different clutches of embryos (**c–e**).



**Extended Data Figure 9 | Aortic *Tp1:GFP* expression is restored by overexpression of *dlc* or *dld* in *jam1a* morphants.** a–h, The aortic expression of *notch1b*, *notch3*, *dlc*, and *dll4* in uninjected or *jam1a* MOatg-injected embryos at 26 hpf. Arrowheads indicate the dorsal aorta (DA). i–p, Lateral views of the DA in *Tp1:GFP* (i–l) and transverse sections of *Tp1:GFP*; *fli1:DsRed* (m–p) at 28 hpf. Embryos were uninjected, injected with *jam1a* MOatg alone,

or co-injected with *jam1a* MOatg and *dlc* or *dld* mRNA. Arrows indicate relatively low activation of *Tp1:GFP* in the ventral floor of the DA. The expression of *Tp1:GFP* was restored in the ventral floor of the DA by co-injection with *dlc* or *dld*. Bars, 10  $\mu$ m. Data are representative of two independent experiments with two different clutches of embryos (a–h), eight embryos (i–l), or three embryos (m–p).



**Extended Data Figure 10 | A model of Notch signal transduction in HSC precursors.** Jam1a<sup>+</sup> PLM cells initially flank the somites then migrate to the midline along the ventral face of the somite, where Jam2a and the Notch ligands Dlc and Dld are expressed. Binding of Jam1a and Jam2a *in trans* is required for transmission of Notch signals into the PLM derivatives that subsequently

generate aortic haemogenic endothelium (left side). In *jam1a*-deficient embryos, although PLM cells arise and initially migrate normally, their migration is delayed upon contact with the somite. Moreover, they show low activation of Notch signalling due to poor interaction with the somite, resulting in the failure of HSC specification in the aortic floor (right side).